UNIVERSITY OF SÃO PAULO

INSTITUTE OF GEOSCIENCES

FERNANDA COSTA GONÇALVES RODRIGUES

Origin and chronology of sandy substrates supporting open vegetation ecosystems in Amazonia

São Paulo

2022

UNIVERSITY OF SÃO PAULO

INSTITUTE OF GEOSCIENCES

Origin and chronology of sandy substrates supporting open vegetation ecosystems in Amazonia

FERNANDA COSTA GONÇALVES RODRIGUES

Ph.D. Thesis presented to the Geochemistry and Geotectonic Graduate Program at the Institute of Geosciences, University of São Paulo, Brazil, to obtain the degree of Doctor of Science.

Concentration area: Geotectonic

Supervisor: Prof. Dr. André Oliveira Sawakuchi

São Paulo

2022

Serviço de Biblioteca e Documentação do IGc/USP
Ficha catalográfica gerada automaticamente com dados fornecidos pelo(a) autor(a) via programa desenvolvido pela Seção Técnica de Informática do ICMC/USP

Bibliotecários responsáveis pela estrutura de catalogação da publicação:
Sonia Regina Yole Guerra - CRB-8/4208 | Anderson de Santana - CRB-8/6658

Costa Gonçalves Rodrigues, Fernanda
Origin and chronology of sandy substrates supporting open vegetation ecosystems in Amazonia / Fernanda Costa Gonçalves Rodrigues; orientador André Oliveira Sawakuchi. -- São Paulo, 2022.
92 p.

Tese (Doutorado - Programa de Pós-Graduação em Geoquímica e Geotectônica) -- Instituto de Geociências, Universidade de São Paulo, 2022.

1. Luminescence dating. 2. Amazonia sandy terrains. 3. Fluvial deposits. 4. Landscape evolution. 5. Open vegetation ecosystems. I. Oliveira Sawakuchi, André , orient. II. Título.

Acknowledgements

First and foremost, I thank my family, especially my mom Malu, for always being by my side, no matter what. You have always supported me through thick and thin and made me persevere to reach my goals.

To my supervisor, André Sawakuchi, many thanks for all opportunities, support, understanding and contributions. To Naomi Porat, for all the guidance, support and patience. To both of you, for your friendship and for believing in me more than I believed in myself.

To Paulo Giannini, thank you for always listening to me, and for all your contributions to my scientific journey, that started with you.

To Thays, Luciana, Ian and Patrícia, for all the laughs, all the help, everything. To all my friends, that in one way or the other contributed to this journey. I don't have words to describe how important you were and are.

To the many colleagues that helped me build this: Fabiano, Camila, Thomas, Julio, João Paulo, Cristiano, Pontien, Jordana, Alexandre, and so many more.

To the Amazonian Biodiversity Studies Centre (CENBAM) and the National Institute for Amazonian Research (INPA) for their support during the fieldwork and permits for sampling in the Negro River Reserve for Sustainable Development (RDS Rio Negro) and Campina Reserve.

To CAPES and FAPESP for the financial support (grants: #2018/12472-8, #2018/23899-2, #2016/02656-9; #2018/15123-4).

To the Institute of Geoscience (University of São Paulo) for all the support and infrastructure throughout my research.

Abstract

RODRIGUES, F. C. G. **Origin and chronology of sandy substrates in Amazonia: implications for Quaternary evolution of open vegetation ecosystems**. 2022. 91p. Ph.D. Thesis – Geochemistry and Geotectonic Graduate Program, Institute of Geosciences, University of São Paulo.

The Amazonia biome hosts upland closed and open vegetation ecosystems, in which the current biogeographical patterns are intricately linked to changes of the physical landscape. Open vegetation ecosystems, especially white-sand ecosystems (WSE) and savannas, have long been thought as key environments of biotic diversification in Amazonia. Understanding the origin, resilience and dynamics of the substrates supporting different ecosystems is indispensable for better comprehension of Amazonian biogeography. Here we investigate the spatial distribution of Amazonian open vegetation ecosystems and their physical landscape, represented relief and type and age of geological substrates. To achieve this aim, we selected sandy substrates areas in central and eastern Amazonia, which were characterized through the application of (i) optically stimulated luminescence (OSL) and thermally transferred (TT) OSL dating, (ii) OSL and thermoluminescence (TL) sensitivity analyses as sedimentary history tracer, (iii) textural and compositional analyses (i.e., grain size, X-ray fluorescence (XRF) and magnetic susceptibility), combined with (iv) a comprehensive review on the substrate origins of different open vegetation ecosystems across Amazonia. Open vegetation ecosystems in Amazonia can be divided as occurring in highland or lowland areas. In the highlands, long-term exhumation and weathering of pre-Cenozoic rocks render more stable upland areas over time. Whereas in lowland Amazonia, the rapidly changing landscape due to the fluvial and eolian systems dynamics can expand or retract sandy substrates and their overlying open vegetation more frequently. The widespread occurrence of savannas and WSE upon the extensive sandy alluvial plains in Negro and Branco Rivers basins are associated to high permeability and repeated rising and falling of the water table, favoring the development of spodosols in that area. These sandy substrates present luminescence ages ranging from almost 2 Ma to 0.9 ka. These ages are discussed in terms of potential geomorphic processes leading to the formation of substrates (solar resetting by soil mixing processes and surface transport or apparent age of the parent bedrock). TT-OSL ages ranging from 2 Ma to 23 ka were primarily interpreted as depositional ages of fluvial sediments, which formed upland terraces after channel incision. OSL ages ranging from 68 ka to 0.9 ka can be interpreted as sedimentation ages or solar resetting by soil processes. OSL equivalent dose distributions with high overdispersion, and overall constancy in grain size statistics, BOSL and TL sensitivities and Zr/Ti and Zr content suggest homogenization of sandy substrates via soil mixing processes. In this case, luminescence ages would represent minimum dates for sandy

substrate development. However, the possibility of such ages representing the time of sand deposition cannot be ruled out. The coupling between OSL and TT-OSL dating techniques allow us to date sedimentary deposits covering the whole Quaternary, which implies a new time window for the Amazonia history. The availability of sandy substrates supporting open vegetation ecosystems change in multiple spatiotemporal scales, and depends on local conditions, such as water table depth, surface elevation and primary sediment grain size, which can lead to decoupling between regional climate patterns and spatial distribution of open vegetation ecosystems. Thus, the development of sandy substrates would rely on local geological controls, favoring open vegetation ecosystems with fragmented spatial distribution and varied temporal persistence.

Keywords: Luminescence dating, Amazonia sandy terrains, Fluvial deposits, Landscape evolution, Open vegetation ecosystems

Resumo

RODRIGUES, F. C. G. **Origem e cronologia de substratos arenosos da Amazônia: implicações para a evolução quaternária de ecossistemas de vegetação aberta**. 2022. 91p. Tese de Doutorado – Programa de Pós-Graduação em Geoquímica e Geotectônica, Instituto de Geociências, Universidade de São Paulo.

O bioma amazônico abriga tanto ecossistemas de vegetação fechada quanto aberta, em que os padrões biogeográficos atuais se relacionam intimamente a mudanças da paisagem física da área. Ecossistemas de vegetação aberta, especialmente os ecossistemas de areia branca (EAB) e as savanas, são considerados como ambientes chave para a diversificação biótica na Amazônia. Entender a origem, resiliência e dinâmica dos substratos que suportam os diferentes ecossistemas é indispensável para melhor compreensão da biogeografia amazônica. Nesta tese, investigamos a distribuição dos ecossistemas de vegetação aberta da Amazônia e as características de sua paisagem física, representadas pelo relevo e tipo e idade do substrato geológico. Para tanto, foram selecionados substratos arenosos na Amazônia central e leste, que foram caracterizados através da aplicação de (i) datação por luminescência opticamente estimulada (LOE ou OSL na sigla em inglês) e LOE termalmente transferida (TT-OSL na sigla em inglês), (ii) análises de sensibilidade LOE e de termoluminescência (TL) como traçadores da história sedimentar dos depósitos, (iii) análises texturais e composicionais (i.e. granulometria, fluorescência de raios-X (FRX) e susceptibilidade magnética), combinados com uma revisão extensiva da literatura sobre a origem dos diferentes substratos de diferentes ecossistemas de vegetação aberta espalhados pela Amazônia. Os ecossistemas de vegetação aberta na Amazônia podem ser divididos entre os que ocorrem nas áreas altas e aqueles nas áreas baixas. Nas áreas altas, os processos mais longos de exumação e intemperismo de rochas pré-Cenozoicas criam áreas de terra firme mais estáveis ao longo do tempo. Já nas áreas baixas da Amazônia, a mudança rápida na paisagem devido à dinâmica dos sistemas fluviais e eólicos cria condições para que os ecossistemas de vegetação aberta possam expandir ou retrair mais rapidamente. A maior ocorrência de savanas e EAB sobre as planícies aluviais arenosas nas bacias dos rios Negro e Branco é associada à alta permeabilidade dos substratos e à subida e descida repetida do nível d'água, que favorece a formação de espodossolos nessa área. Tais substratos arenosos apresentam idades de luminescência variando de 2 Ma até 0.9 ka. Estas idades são discutidas em termos dos processos geomórficos potenciais que formaram os substratos (fotoesvaziamento devido à processos de mistura de solo ou transporte de grãos em superfície ou idade aparente do substrato rochoso fonte). As idades TT-OSL (variando de 2 Ma até 23 ka) foram interpretadas primariamente como idades deposicionais de terraços fluviais após incisão. As idades OSL (variando de 68 a 0.9 ka) podem ser interpretadas tanto como idades deposicionais quanto fotoesvaziamento por processos de mistura do solo. A distribuição larga dos valores de doses equivalentes OSL e a consistência nas estatísticas de

tamanho de grão, sensibilidade OSL e TL e conteúdo de Zr/Ti e Zr sugere homogeneização por mistura do solo. Entretanto, a possibilidade de tais idades indicarem o momento de deposição não pode ser descartada. A associação das técnicas de datação OSL e TT-OSL permite a datação de depósitos sedimentares abrangendo todo o período do Quaternário, o que implica em uma nova janela de tempo para a história da Amazônia. A disponibilidade de substratos arenosos que suportam ecossistemas de vegetação aberta muda em múltiplas escalas espaço-temporais, e depende de condições locais, como nível d'água, elevação e tamanho de grão, o que pode gerar uma dissociação entre os padrões de clima regional e a distribuição espacial dos ecossistemas de vegetação aberta. Assim, o desenvolvimento dos substratos arenosos dependeria de controles geológicos locais, favorecendo a fragmentação espacial e variada resiliência temporal dos ecossistemas de vegetação aberta.

Palavras-chave: Datação por luminescência, terrenos arenosos da Amazônia, Depósitos fluviais, Evolução da paisagem, Ecossistemas de vegetação aberta

Thesis outline

The Amazonia is known worldwide for its high biodiversity and large transcontinental river system. Changes in the physical landscape, like drainage expansion and shifting between seasonally flooded and upland terrains, are recognized as an important driver of biotic diversification. Previous studies have focused on the role of rivers and the formation of fluvial substrates holding upland (*terra-firme*) forests for the Amazonian biota diversification (e.g. Ayres and Clutton-Brock, 1992; Cracraft, 1985; Ribas et al., 2012). However, Amazonia also hosts several patches of open vegetation, including white-sand ecosystems and savannas upon sandy substrates. Such open ecosystems presumed played a significant role for biotic diversification of upland forest species, host endemic and specialist species and have long been on the center of the discussion on Amazonian species evolution (e.g. Haffer, 1969). Given the marked importance of the physical landscape on creating the high biodiversity seen today in Amazonia, this thesis aims to understand the spatial distribution of open vegetation ecosystems and characteristics of their sandy substrates. Specific areas hosting sandy substrates in eastern and central Amazonia were selected for characterization, through the combination of methods, which included (i) quartz optically stimulated luminescence (OSL) and thermally transferred (TT)-OSL chronology, (ii) quartz OSL and thermoluminescence (TL) sensitivity analyses as sedimentary history tracer, (iii) textural and compositional analyses, such as grain size, X-ray fluorescence (XRF) and magnetic susceptibility, and (iv) a comprehensive review on the spatial distribution and substrate types of different open vegetation ecosystems across Amazonia.

This thesis is composed of four chapters. *Chapter 1* presents the scientific background on Amazonia open vegetation ecosystems and the relationship between biotic diversification and landscape changes, as well as the specific goals set for this doctoral research. *Chapter 2* addresses the application of quartz luminescence extended-age dating technique (TT-OSL) of fluvial deposits in closed and open vegetation environments in central and Eastern Amazonia. This is crucial to address landscape changes beyond the late Pleistocene, which is a limitation of published geochronological dataset aiming to constrain the Quaternary landscape history of Amazonia. *Chapter 3* discusses the origin, temporal variation and stability of the sandy substrates supporting Amazonian open vegetation ecosystems. *In Chapter 4*, the summary and main conclusions from Chapters 2 and 3 are presented. The manuscripts presented in Chapters 2 and 3 are individually understandable and are either accepted for publication or in preparation for submission in peer-reviewed scientific journals:

- **Chapter 2** – *Extended-range luminescence dating of central and eastern Amazonia sandy terrains*; accepted for publication in Frontiers in Earth Sciences Special Volume "Landscape Evolution of the Tropical Regions: Dates, Rates and Beyond", on June 13rd, 2022.

- **Chapter 3** – *Geological controls upon formation and distribution of open vegetation ecosystems in Amazonia*; manuscript in preparation for submission.

Moreover, the appendixes of this thesis include the supplementary material of both manuscripts presented in Chapters 2 and 3:

- **Appendix 1** – Supplementary material for "*Extended-range luminescence dating of central and eastern Amazonia sandy terrains"*; accepted for publication in Frontiers Special Volume "Landscape Evolution of the Tropical Regions: Dates, Rates and Beyond", on June 13rd, 2022.
- **Appendix 2** – Supplementary material for "*Geological controls upon formation and distribution of the open vegetation ecosystems in the Amazonia"*; in preparation for submission.

Table of Contents

1 Introduction

1.1 Scientific background and motivation

The remarkable biodiversity of the Amazonia biome and its drivers have puzzled researchers over decades, with many hypotheses proposed to explain the historical processes that shaped current biogeographical patterns (e.g. Bush, 1994; Colinvaux, 1987; Haffer, 1969; Jaramillo et al., 2006; Nelson et al., 1990; Rull, 2008). Most hypotheses include the formation of barriers to gene flow due to changes in climate (e.g. refuge hypotheses; Haffer, 1969) or in the landscape associated with fluvial activity c); mountain formation (Hoorn et al., 2013; Luebert and Muller, 2015) and marine incursions (Bates, 2001). Knowledge about changes of physical landscape through time is crucial to understand their relation to the current biodiversity and biogeographical patterns of the biome, and to do so reliable chronology to constrain the formation of terrains occupied by different Amazonian ecosystems are needed.

Recent studies have been focusing on the role of rivers for the Amazonian biota diversification. The formation of a transcontinental drainage system and the evolution of its contributary systems, that transformed flooded forests (*várzeas* and *igapós*) into upland forests (*terra firme* forests), are regarded as a main factor of Amazonian biota diversification (Hoorn and Wesselingh, 2010; Ribas et al., 2012). Despite the common sense see Amazonia as a homogeneous dense rainforest, it hosts unique patches of open vegetation, including white-sand ecosystems (WSE) and savannas. These open vegetation ecosystems also played an important role in the biota diversification, since they house different endemic and/or specialists' species (Alonso, 2002; Alonso et al., 2013; Anderson, 1981; Borges, 2004; Borges et al., 2016, 2015; Fine et al., 2010), occupying the core of the debate about climatic drivers of biotic diversification in Amazonia for decades (e.g. Anhuf et al., 2006; Haffer, 1969; Sato et al., 2021).

In the late 1960s, Haffer (1969) proposed the Refugia Hypothesis, stating that Amazonia biodiversity results from allopatric speciation, due to genetic isolation of islands of forests (the refugia) surrounded by widespread savannas during the Last Glacial Maximum (LGM) around 21 ka ago. Ever since its publication, many studies have risen both supporting (e.g., Haffer, 1985, 1990; Haffer & Prance, 2001; Van Der Hammen and Hooghiemstra, 2000; Anhuf et al., 2006) and denying (Colinvaux et al., 2000; Bush et al., 2004; Mayle et al., 2004; Bush & Oliveira, 2006) such vegetational cover change in the LGM. Within this context of savanna expansion, phylogenetic studies have shown demographic expansion of WSE specialist birds ever since the LGM (Capurucho et al., 2013; Matos et al., 2016), indicating an increase of open vegetation habitats availability and connectivity.

Like the variety of ecosystems within the Amazonia biome, there is a great variety of geological substrates supporting these different ecosystems. As the seasonally flooded forests are

related to the floodplain areas within river valleys and the upland forests to the interfluves (Sioli, 1984), open vegetation ecosystems occur on bare rock of the Guiana and Central Brazil shields (Rull et al., 2019), upon eolian deposits on the Negro and Branco rivers basins (Sinha, 1968; Eden & McGregor, 1992; Carneiro Filho & Zinck, 1994; Schaefer and Dalrymple, 1995; Latrubesse & Nelson, 2001; Carneiro Filho et al., 2002; Teeuw & Rhodes, 2004; Zular, 2016), on alluvial fans and fluvial deposits along the Madeira and Negro rivers basins (Rossetti et al., 2019, 2017a, 2017b, 2014, 2012a, 2012b; Zani and Rossetti, 2012) and on hydromorphic spodosols in the Negro River basin (Adeney et al., 2016). Therefore, hypotheses about the origin of Amazonian open vegetation terrains are diverse and vary regionally and few studies present absolute ages to constrain the timing of their development or their formation processes (Carneiro Filho et al., 2002; Rossetti et al., 2019; Zular et al., 2019).

The Holocene and Late Pleistocene history of the lowland Amazonia fluvial landscape has been better understood thanks to reliable radiocarbon and optically stimulated luminescence (OSL) dating of quartz of fluvial deposits (e.g., Cremon et al., 2016; Pupim et al., 2019; Rossetti et al., 2015). Yet, many environments related to Early and Middle Pleistocene and Pliocene sedimentary deposits in lowland Amazonia remain a mystery, due to lack of studies or due to the challenge of extended-age dating protocols beyond the Late Pleistocene in heavily weathered siliciclastic and non-fossiliferous deposits.

This doctoral research shows new data recording the chronology of sandy substrates in Amazonia and their possible formation processes. We investigated sandy substrates supporting both open and closed vegetation ecosystems in central and eastern Amazonia, through the combination of (i) OSL and thermally transferred (TT)-OSL chronology, (ii) quartz luminescence sensitivity analyses, and (iii) textural and compositional analyses, such as grain size, X-ray fluorescence (XRF) and magnetic susceptibility. Data from this suite of analytical methods was used to improve our understanding on the timing and origin of these sandy substrates supporting different ecosystems across Amazonian uplands.

1.2 Objectives

Starting from the observation that many open vegetation ecosystems occur upon sandy substrates, it is assumed that the expansion and/or retraction of these ecosystems is intimately linked to the formation dynamics of sandy substrates. Therefore, these substrates constitute potential records of the open vegetation ecosystems development.

The main goal of this doctoral research is to understand the origin and spatiotemporal dynamics of Amazonian open vegetation ecosystems substrates, including their resilience through time, especially during the Quaternary. To investigate this, the following goals were addressed:

I) Identification of open vegetation ecosystems distribution according to characteristics of the Amazonia physical landscape (geological patterns, relief and precipitation);

II) Establishment of reliable chronology of sandy substrate formation, using quartz OSL and TT-OSL dating, in different open and closed vegetation substrates;

III) Evaluation of surface processes leading to the formation of sandy substrates using a suite of textural and compositional analyses (grain size, XRF, magnetic susceptibility and luminescence sensitivity);

IV) Understand major controls on the distribution of sandy substrates in Amazonia across space and time.

1.3 Environmental setting

1.3.1 Amazonia biome: open vegetation ecosystems

The Amazonian biome is composed of upland (*terra-firme*) ecosystems not exposed to seasonal flooding (86%) and seasonally flooded ecosystems (14%) (Hess et al., 2015). Within the uplands, the main open vegetation ecosystems are the Pantepui, Guianna savannas, WSE and smaller savanna patches, referred to as "*campos/cerrado*" (Adeney et al., 2016). Within the seasonally flooded ecosystems, the Beni savannas stand out as the open vegetation ecosystem (Adeney et al., 2016).

The Pantepui ecosystem hosts a high level of endemism and richness of vascular plants, and is dominated by meadows, shrublands and woodlands growing on peat and bare rocks (Rull et al., 2019). Forests occur restricted to depressions and water courses and are usually low and species-poor (Rull et al., 2019). This ecosystem occurs in the table-top mountains in northern Amazonia, over 1000 m in elevation, isolated from the ground forest. The Guianna savannas and smaller savanna patches spread out through Amazonia are tropical mixed tree-grass systems (Eiten, 1986; House et al., 2003; Huber, 1987; Sarmiento, 1984; Scholes and Archer, 1997), occupying 268 × 10^3 km^2 of the Amazonia biome (Adeney et al., 2016; Carvalho & Mustin, 2017). WSE include zones dominated by open or closed vegetation, usually grading from one to another. Usually, WSE are species-poor with high endemism (Anderson, 1981). The main ecological correlate between the many types of white-sand vegetation resumes to the quartz-rich sandy soil that these ecosystems develop upon (Adeney et al., 2016). Beyond the soil type, WSE is also associated to impeded drainage (Adeney et al., 2016). The Beni savannas occur in Bolivian Amazonia and are shaped by drought and flood dynamics of the Madeira River watershed. This ecosystem is formed by herbaceous wetlands, grasslands, woodlands, and isolated patches of evergreen forests (Borghetti et al., 2020).

1.3.2 Geological framework of Amazonia

The Amazonia biome lies upon the Andes orogen and its associated Cenozoic foreland basins, pre-Cambrian crystalline rocks and Paleozoic-Mesozoic cratonic basins. The Amazonian Craton eastward of Andes comprises the Guianna Shield (northern Amazonia) and the Central Brazil Shield (southern Amazonia), and is composed of a complex arrangement of igneous and metamorphic rocks dated at 3.4 – 1.9 Ga, sandstones and conglomerates of ~1.8 Ga and felsic and mafic volcanic rocks dated at 1.5 – 1.8 Ga (Briceño and Schubert, 1990; Coutinho, 2008; Voicu et al., 2001). The Amazonia comprises 13 sedimentary basins: Beni, Madre de Dios, Ucayali, Acre, Putumayo, Llanos, Solimões, Amazonas, Marajó, Parecis, Alto Tapajós, Xingu and Parnaíba (Gómez Tapias et al., 2019).

The geological history of Amazonia during the Cenozoic is recorded mostly by widespread fluvial deposits. In western and Central Amazonia, the Solimões Formation records fluvial systems from the Miocene (Latrubesse et al., 2010), with possible marine incursions from north (Jaramillo et al., 2017), and is partially correlated to the Pebas Formation in Peru and Colombia. The Solimões Formation in the Acre Basin is regarded as a large wetland developed previously to the transcontinental Amazon River (e.g. Latrubesse et al., 2010; Wesselingh and Salo, 2006). In early Pliocene (~5 Ma), sedimentary basins of western Amazonia were filled forcing fluvial systems draining eastward (Hoorn and Wesselingh, 2010) and originating the current watershed of the Amazon River at 6.8-2.4 Ma (Figueiredo et al., 2009). The Içá Formation lies upon the Solimões Formation, deposited by a meandering fluvial system from 6.8 to 2.4 Ma (Horbe et al., 2013; Roddaz et al., 2005). Pupim et al. (2019) obtained luminescence ages from 250 to 45 ka for the Içá Formation deposition, suggesting a major phase of fluvial aggradation during the Middle and Late Pleistocene followed by a continued erosion and channel incision since the late stages of the Late Pleistocene.

In central Amazonia, ancient fluvial systems are recorded by the Alter do Chão Formation, Iranduba and Novo Remanso Formations. The lower boundary of Alter do Chão Formation hosts palynological data of the late Cretaceous (Dino et al., 2012, 1999). However, its upper boundary can reach the Paleogene (Caputo, 2011; Gautheron et al., 2022). The Iranduba Formation lies unconformably upon the the Alter do Chão Formation and there is no specific chronological control for its deposition so far. The Novo Remanso Formation sits upon the Iranduba Formation and is regarded as a Neogene fluvial record, spanning from the middle Miocene to the Pliocene (Guimarães et al., 2015; Gautheron et al., 2022). The Alter do Chão, Iranduba and Novo Remanso Formations are composed mostly of sandstones, contrasting with westward correlative stratigraphic units, which host siginificant fine-grained facies.

1.3.3 Amazonia climate

The South American monsoon system (SAMS) is responsible for rainfall over Amazonia (Zhou and Lau, 1998). Seasonal rainfall variations depend on the dynamics the Intertropical Convergence Zone (ITCZ), whose latitudinal position over the Equatorial Atlantic drive the inland transport of moisture to activate the SAMS. During the austral summer, the strengthening of the SAMS increases precipitation rainfall over the Amazon drainage basin (Zhou and Lau, 1998). Interannual rainfall anomalies are caused by El Niño – Southern Oscillation (ENSO), that promotes drier and wetter periods in the Amazon basin during strong El Niño and La Niña events, respectively (Bookhagen and Strecker, 2010; Garreaud et al., 2009; Hoffmann et al., 2003; Vuille et al., 2003). Interannual anomalies are also related to changes in sea surface temperature in the Atlantic (Espinoza et al., 2014; Marengo et al., 2012, 2008; Yoon and Zeng, 2010). In the millennial-scale, slowdowns in the Atlantic meridional overturning circulation (AMOC) decreased precipitation over northern Amazonia, and increased precipitation over western and eastern Amazon basin (Crivellari et al., 2018; Kanner et al., 2012; Zhang et al., 2017). Changes in insolation due to precession cycles (~23 ka) are responsible for marked changes in Amazonian rainfall, when intervals of high austral summer insolation intensify the SAMS (Cheng et al., 2013; Govin et al., 2014).

2 Extended-range luminescence dating of Central and Eastern Amazonia sandy terrains

FERNANDA COSTA G. RODRIGUES, Naomi Porat, Thays Desiree Mineli, Ian Aitor Del Río, Pontien Niyonzima, Luciana Nogueira, Fabiano do Nascimento Pupim, Cleverson Guizan Silva, Paul Baker, Sherilyn Fritz, Ingo Wahnfried, Gustavo Kiefer, André Oliveira Sawakuchi

2.1 Abstract

The Amazonia biome hosts upland closed and open vegetation ecosystems, in which the current biogeographical patterns relate to the evolution of the physical landscape. Therefore, understanding the origin and timing of the substrates supporting different ecosystems is indispensable for better comprehension of Amazonian biogeography. Here we used quartz optically stimulated luminescence (OSL) and thermally transferred optically stimulated luminescence (TT-OSL) for dating sandy substrates of closed and open vegetation environments in Central and Eastern Amazonia, from both outcrop and drill core samples (Autazes core: PBAT-15-43). These sandy substrates present ages ranging from 1 ka up to almost 2 Ma, that were primarily interpreted as depositional ages of fluvial terraces. Moreover, ages are discussed in terms of potential geomorphic processes leading to the formation of substrates, such as soil mixing and apparent age of quartz from the parent bedrock. The coupling between OSL and TT-OSL techniques allow us to date sedimentary deposits covering the whole Quaternary, which implies a new time window for the Amazonia history.

2.2 Introduction

The evolution of Amazonian biota and its remarkable biodiversity are intricately linked to the evolution of the physical landscape, and the formation of the transcontinental drainage system is proposed as a main driver for biotic diversification within the Amazonian biome (Boubli et al., 2015; Hoorn et al., 2010; Ribas et al., 2012). In addition to the well-known closed upland rainforest, Amazonia also hosts isolated patches of open vegetation, such as savannas and white-sand ecosystems (WSE) (Adeney et al., 2016; Anderson, 1981), which are considered important environments that drove biodiversification in upland Amazonia (Haffer, 1969) and other ancestral regions (Frasier et al., 2008). Therefore, extended-range chronologies of sedimentary substrates supporting upland vegetation in Amazonia are crucial to understand the evolution of the landscape during the Quaternary and Neogene and its relation to the current biodiversity and biogeographical patterns of the biome. The Pliocene and Quaternary lowland fluvial record in Central Amazonia is composed of heavily weathered siliciclastic and non-fossiliferous deposits, suitable for the application of quartz-based dating techniques (e.g., Bezerra et al., 2022; Pupim et al., 2019; Soares et al., 2010), as feldspar is frequently lacking due to heavy weathering. Most of the reliable ages that constrain sedimentation in these sequences are based on optically stimulated

luminescence (OSL) dating of quartz (e.g., Cremon et al., 2016; Pupim et al., 2019; Rossetti et al., 2015) and are restricted to the last 300 ka.

OSL is the light arising from charges trapped in crystal lattice defects when quartz is exposed to ionizing radiation and subsequently released and recombined when quartz is exposed to stimulation light. Measuring the natural OSL signal allows the determination of radiation dose absorbed by quartz during burial, and sediment depositional ages are estimated by dividing the radiation dose (Gy) by the environmental dose rate (Gy/ka). Several extended-range luminescence dating methods were proposed with the potential to date as far as the Early Pleistocene, including thermally transferred optically stimulated luminescence (TT-OSL), with reported equivalent dose (D_e) values up to 2500 Gy (Wang et al., 2006a). The TT-OSL signal is measured by depleting the OSL signal, applying a heat treatment ≥260 °C to transfer charges from TT-OSL traps into OSL traps, and remeasuring the OSL signal (Adamiec et al., 2010; Wang et al., 2006a). The charge transfer has been hypothesized as a double transfer, where electrons from OSL traps are released and stored in a refuge trap, before being thermally transferred back (Wang et al., 2006a) or alternatively as a single transfer, where electrons are thermally transferred from a source trap to an OSL trap (Adamiec et al., 2010). The TT-OSL signal is represented as (i) the recuperated OSL (Re-OSL), which makes up about 90% of the signal and is more sensitive to light, and (ii) the basic-transferred OSL (BT-OSL) (Aitken, 1998; Duller and Wintle, 2012), which makes up the remaining 10%. Both multiple-aliquot (MAR) and single-aliquot (SAR) regenerative dose protocols have been proposed to estimate D_e using the TT-OSL signal (e.g., Adamiec et al., 2010; Chapot et al., 2016; Porat et al., 2009; Wang et al., 2006a).

Despite the routine use of TT-OSL dating in recent years, only few studies use this technique in geological settings of South America (e.g., Bezerra et al., 2022; Pupim et al., 2016). In addition to the understating of the evolution of the Amazonian landscape in the Pliocene and Quaternary, TT-OSL dating protocols still need to be tested in different geological contexts, including South America, as quartz OSL properties are not uniform and also vary at a grain-to-grain level (Preusser et al., 2009), and the same might be valid for the TT-OSL signal. In this study, we used both quartz OSL and TT-OSL for dating upland sandy deposits covered by open and closed vegetation in lowland Central and Eastern Amazonia. The formation chronology of these deposits allows us to understand how upland terrains bounding the Amazon River floodplains were assembled in periods beyond the late Pleistocene.

2.3 Study sites and sampling

This study used two datasets from Central Amazonia and two from Eastern Amazonia (Figure 1). The Eastern Amazonia dataset comprises outcrop samples from sandy substrates of savannas exposed in pits and road cuttings, for which the depositional and/or weathering origin is still under

debate. Eastern Amazonia sandy substrates are composed of massive, loose, medium, and poorly to moderately sorted light reddish to brownish sands (AVA01 – Figure 2a and b). The Central Amazonia datasets comprise both outcrop samples from substrates of open vegetation ecosystems (i.e., WSE), composed of massive, loose, and coarse white sands (AVA22 – Figure 2c and d), and drill core samples composed of heavily weathered fluvial sandstones and siltstones (Autazes Core: PBAT-15-43, Figure 2e and f). These sand substrates cover Pliocene-Miocene and late Cretaceous-Paleogene fluvial deposits from the Novo Remanso and Alter do Chão Formations (Gautheron et al., 2022).

Outcrop samples were collected in aluminum or opaque PVC tubes to avoid sunlight exposure. Drill core samples were wrapped in aluminum foil, and only the inner sections were used for luminescence analysis while the outer section exposed to light was used for determination of radionuclides concentrations needed for dose rate estimation. Sediments within a radius of 30 cm from the luminescence sampling point in the outcrops were collected separately to estimate radiation dose rates.

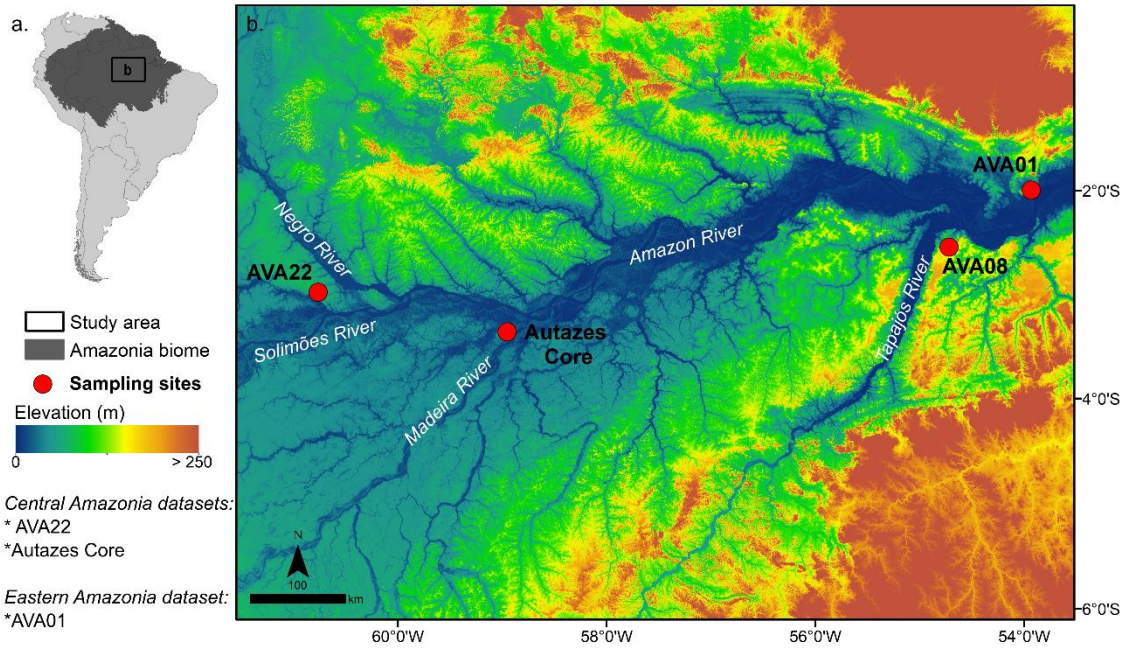

Figure 1: (a) Location of the Amazonia biome within South America and study area within this biome; (b) digital elevation model (DEM; from Shuttle Radar Topography Mission - SRTM) and sampling locations in Central (AVA22 and Autazes core) and Eastern (AVA01 and AVA08) lowland Amazonia.

Figure 2: (a) AVA01 outcrop in Eastern Amazonia with savanna sandy substrate covering late Cretaceous-Paleogene sandstones from the Alter do Chão Formation (dashed black line indicates the upper boundary of the Alter do Chão sandstones); (b) close-up image of the savanna sandy substrate in AVA01; (c) AVA22 outcrop of sandy deposits covered by white-sand vegetation (*campina*) in Central Amazonia; (d) close up image of the sandy substrate of white-sand vegetation; (e) Autazes drill core weathered sandstones and siltstones from 0 to 10.42 m depth (from left to right), (f) Autazes drill core weathered sandstones and siltstones from 10.42 to 18.85 m depth (from left to right).

Table 1: Summary information of samples used in this study.

	Sampling	Sample Code	Lab Code	Latitude	Longitude	Depth (m)
Eastern Amaz.	Outcrop	AVA01C	L1083	-2.009195°	-54.094106°	0.5
		AVA01E	L1084	-2.009195°	-54.094106°	1.0
		AVA01G	L1085	-2.009195°	-54.094106°	1.5
		AVA08B	L1106	-2.553336°	-54.960837°	1.0
Central Amazonia	Outcrop	AVA22A	L1436	-3.115015°	-60.746138°	0.8
		AVA22C	L1438	-3.115015°	-60.746138°	1.4
		AVA22E	L1440	-3.115015°	-60.746138°	2.0
	Autazes core (PBAT-15-43)	155812	L1490	-3.494253°	-58.973555°	0.2
		155813	L1491	-3.494253°	-58.973555°	1.8
		155814	L1492	-3.494253°	-58.973555°	2.7
		155815	L1493	-3.494253°	-58.973555°	4.9
		155816	L1488	-3.494253°	-58.973555°	5.8
		155817	L1487	-3.494253°	-58.973555°	6.6
		155818	L1486	-3.494253°	-58.973555°	11.4
		155819	L1485	-3.494253°	-58.973555°	13.7

2.4 Sample preparation and measurements

Sample preparation and measurements were carried out under subdued orange-red light. The preparation procedures of quartz concentrates included wet sieving to separate the 180–250 μm fraction; dissolving organic matter with 35% H_2O_2 and carbonates with 10% HCl solutions; density separation at 2.75 g/cm^3 and 2.62 g/cm^3 with lithium metatungstate (LMT) solution to

isolate quartz grains from heavy minerals and feldspar grains; and etching in concentrated 40% HF solution for 40 minutes to eliminate the outer rind of quartz grains affected by alpha radiation and remnant feldspar grains. Density separation showed that little to no feldspar was present in the studied samples.

All measurements were performed using two Risø DA-20 TL/OSL readers and a Lexsyg Smart reader, all equipped with $^{90}Sr/^{90}Y$ beta source (dose rates of 0.07, 0.12 and 0.11 Gy/s respectively), blue and infrared LEDs for stimulation, and a 7.5 mm Hoya U-340 filter for light detection in the ultraviolet band. Aliquots of 4 to 9 mm diameter were prepared using adhesive silicone spray on stainless steel discs or cups. OSL-IRSL depletion ratio was used to confirm that there was no feldspar contamination in the quartz aliquots (Duller, 2003).

The SAR protocols used to determine the D_e using the OSL (Murray and Wintle, 2000) and TT-OSL (Porat et al., 2009) signals are described in Table 2. The OSL SAR protocol was also used to estimate the characteristic dose (D_0) of dose response curves, and $2D_0$ was considered to appraise the upper limit for OSL dating in the studied sediment samples (Wintle and Murray, 2006). The intervals used to derive both OSL and TT-OSL signals were the integral of the first 1 s of light emission, minus the last 10 s as background. Dose-response curves (DRC) were fitted using a linear, single saturating exponential, or an exponential plus linear functions. D_e was calculated using the unweighted arithmetic mean (empirical average) of individual dose estimates, as suggested by (Guérin et al., 2017), accepting recycling ratios between 0.9 – 1.1 and 0.8 – 1.2 and recuperation up to 5% and 10%, for OSL and TT-OSL, respectively. The suitability of both OSL and TT-OSL SAR protocols for estimation of D_e under laboratory conditions was evaluated by dose recovery tests (data summary of dose recovery tests on Table S1 and S2). The dose recovery tests performed by Bezerra et al. (2022) on samples from the same study area were also used for evaluation of the suitability of the TT-OSL protocol. OSL average calculated-to-given dose ratio is 0.96, and TT-OSL average calculated-to-given dose ratio is 1.5 (Table S2).

The concentrations of U, Th, and K for determination of dose rates were measured using high-resolution gamma spectrometry with a high-purity germanium detector (Canberra Instruments, relative efficiency of 55% and energy resolution of 2.1 keV at 1332 keV) encased in an ultralow background shield. Inductively coupled plasma mass spectrometry (ICP-MS) was also used for determination of U and Th concentrations and inductively coupled plasma atomic emission spectroscopy (ICP-OES) was used to determine K concentration. U, Th and K concentration uncertainties from gamma spectrometry are 1σ. ICP-MS U and Th uncertainties are 5 % and 10 %, respectively. ICP-OES K uncertainty is 3 %. The concentrations of U (ppm), Th (ppm), and K (%) were converted into dose rates (Gy/ka) using the conversion factors proposed by Guérin et al. (2011). Cosmic rays' contribution to the dose rate was calculated according to Prescott and Hutton (1994), considering the latitude, longitude, altitude, current depth below the surface, and

density of each sample. The internal dose rate was assumed as 0.01 Gy/ka, as this value is considered the upper limit to the internal alpha dose rate in quartz (Vandenberghe et al., 2008).

Table 2: Single-aliquot regenerative-dose (SAR) OSL and TT-OSL protocols used to estimate equivalent doses (D_e) from quartz aliquots in this study. Gray shading indicates steps to measure OSL or TT-OSL signals used to build dose response curves and calculate the D_e.

Step	OSL (Murray and Wintle, 2000)	TT-OSL (Porat et al. 2009)
1	Give dose Di (*natural signal, i = 0 and D0 = natural dose*)	Give dose Di (*natural signal, i = 0 and D0 = natural dose*)
2	Preheat at 240°C for 10 s	Preheat at 260°C for 10 s
3	OSL at 125°C for 40 s (Li)	OSL at 125°C for 200 s
4	Give a test dose of 10 or 25 Gy	Preheat at 260°C for 10 s
5	Preheat at 160°C for 10 s	TT-OSL: OSL at 125°C for 100 s (Li)
6	OSL at 125°C for 40 s (Ti)	Give a test dose of 10 or 50 Gy
7	Blue LED illumination at 280°C for 40 s	Preheat at 200 or 240°C for 10 s
8		OSL at 125°C for 100 s (Ti)
9		Deplete remaining TT-OSL: OSL at 350°C for 100 s

D1 < D2 < D3 < D4, D5 = 0 Gy, D6 = D1, D7 =D1 (with infrared stimulation before blue led stimulation)

2.5 Results

Representative OSL and TT-OSL decay curves and DRC of Eastern and Central Amazonia study sites are shown in Figure 3. All samples have the OSL curve dominated by the fast component in the first 1 s, with the OSL signal decaying slightly slower in Central Amazonia samples. The TT-OSL signal also decays slower in Central Amazonia samples. All samples have saturated natural OSL signals, except for the two shallowest samples of the Autazes Core, at 0.2 m and 1.8 m depth, which have D_e of 4.6 ± 0.5 Gy and 94.6 ± 4.7 Gy, respectively (Table 3), and for sample AVA08, with D_e of 52.3 ± 3.5 Gy. The OSL $2D_0$ of all samples ranges from 90 to 180 Gy (Table 3), indicating the limits of OSL dating. TT-OSL D_e ranges from 92 ± 9 Gy to 1692 ± 229 Gy in Central Amazonia samples and from 161 ± 10 Gy to 747 ± 74 Gy in Eastern Amazonia samples (Table 3 and Figure 5a). Overdispersion of the TT-OSL D_e distribution varies from 16% to 61% (Table 3 and exemplary D_e distribution on Figure 4b, d, and f). All samples have high sensitivity changes meaning that the test dose signal increases with SAR cycles as a response to the same beta dose, with more significant increases occurring on the AVA22 samples (Figure 4a, c, and e). The difference between TT-OSL D_e and OSL D_e for samples AVA08B, 155812, and 155813 is 109 Gy, 87 Gy, and 142 Gy, respectively.

The Autazes core has a trend of increasing D_e with depth, and the Eastern and Central Amazonia outcrop depth profiles (AVA01 and AVA22) present statistically indistinguishable values. Dose rates are lower in the outcrops in Central and Eastern Amazonia (~0.6 Gy/ka) than in the Autazes core (~3.6 Gy/ka) (Figure 5a). All samples have less than 1% of K content, and U is usually higher in Central Amazonia samples (both AVA22 and Autazes core) than in Eastern Amazonia (Figure 5b, c and d and supplementary material). The Th content in the Autazes core is ~20x higher than in the outcrop profiles (AVA01 and AVA22) (Figure 5d and supplementary material). Ages in the Eastern Amazonia AVA01 profile range from 1927 ± 246 ka to 1239 ± 294 ka and ages in the Central Amazonia AVA22 profile range from 1058 ± 198 ka to 923 ± 142 ka (Table 3 and Figure 6). In the Autazes core, the TT-OSL ages obtained are younger than the ages from other outcrop profiles, ranging from 585 ± 85 ka to 23 ± 3 ka (Table 3 and Figure 6).

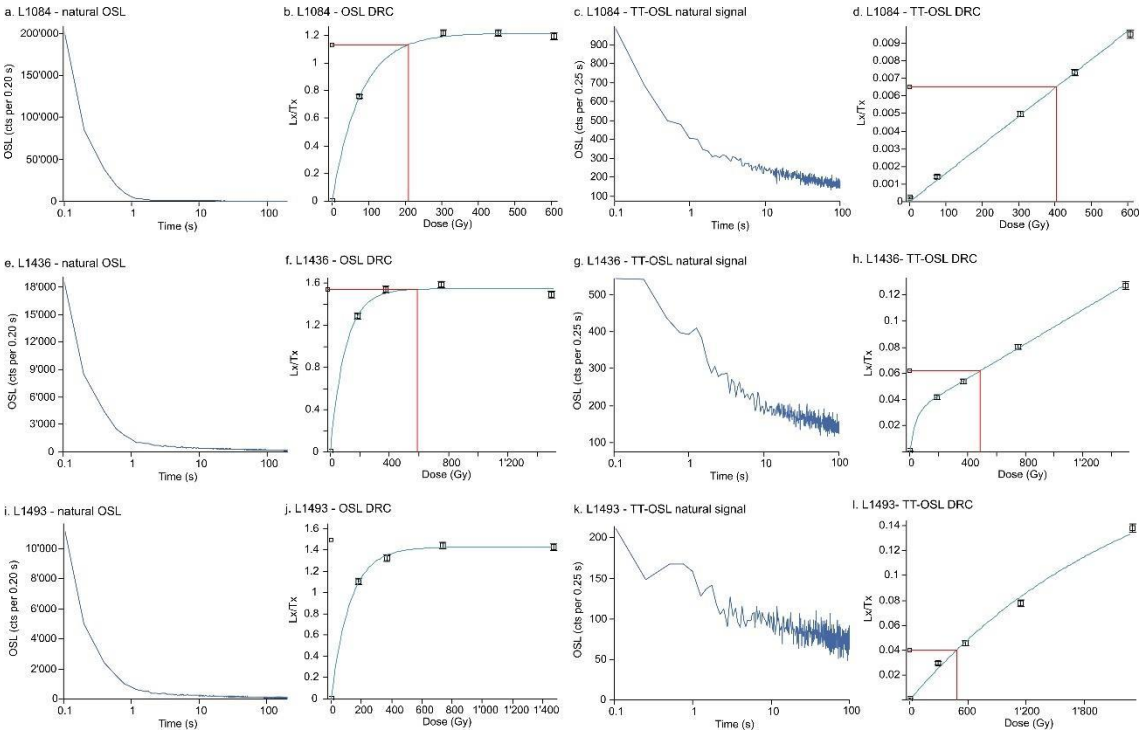

Figure 3: Natural OSL and natural TT-OSL signals of representative samples of the study sites and their respective DRCs. Sample L1084 – outcrop in Eastern Amazonia; sample L1436 - outcrop in Central Amazonia; sample L1493 – Autazes core in Central Amazonia.

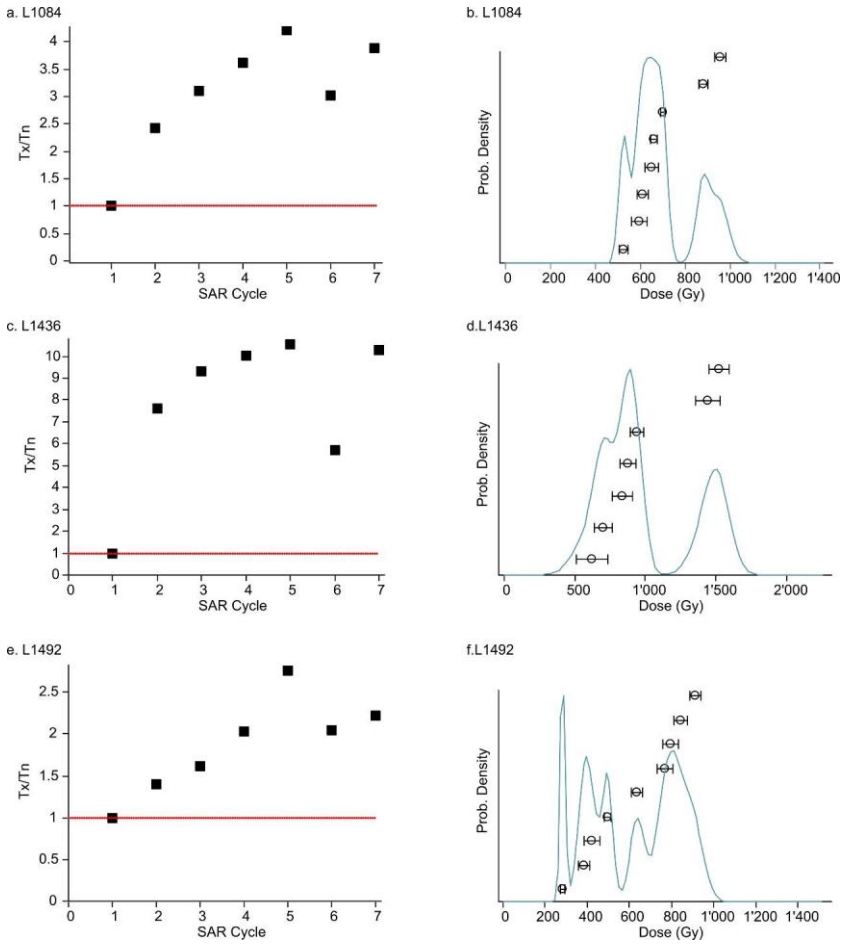

Figure 4: Sensitivity changes over each SAR cycle and TT-OSL D_e distributions of representative samples AVA01E (L1084 – a and b), AVA22A (L1436 c and d), and 155814 (L1492 – e and f).

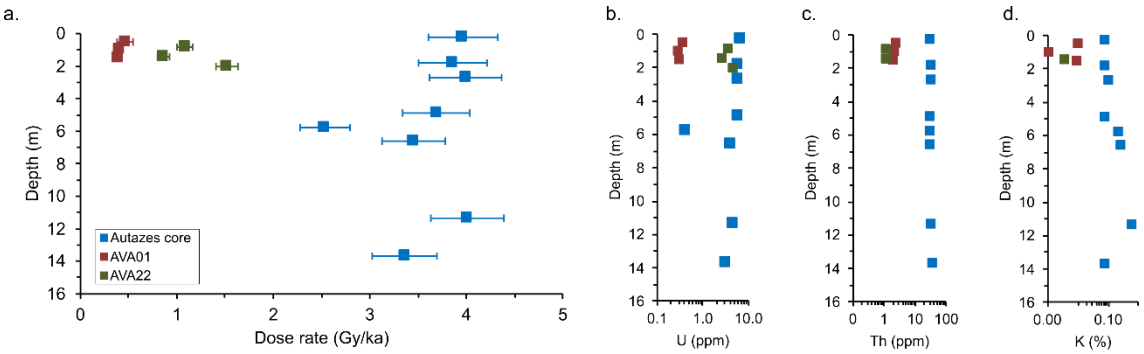

Figure 5: Dose rate (a), U concentration (b), Th concentration (c) and K concentration (d) versus depth in sediment profiles of the study area.

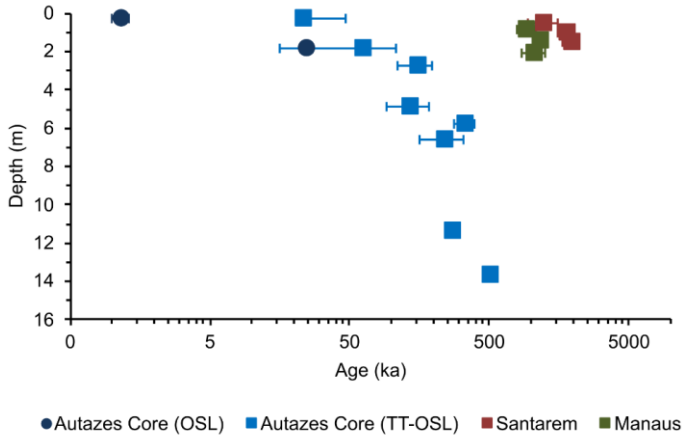

Figure 6: OSL and TT-OSL ages versus depth for the studied samples.

Table 3: Summary of luminescence dating results. Light orange shading indicates TT-OSL D_e and ages, and light blue shading indicates OSL D_e and ages. "OD" is the overdispersion of D_e distributions and "N" is the number of aliquots per sample.

Location	Sample	Lab Code	N	D_e (Gy)	OD (%)	Dose rate (Gy/ka)	Age (ka)	OSL $2D_0$
Eastern Amazonia (outcrop)	AVA01C	L1083	7	562 ± 90	36	0.46 ± 0.08	1239 ± 294	120
	AVA01E	L1084	7	713 ± 57	19	0.41 ± 0.04	1789 ± 237	130
	AVA01G	L1085	8	747 ± 74	23	0.40 ± 0.03	1927 ± 246	105
	AVA08B	L1106	23	52.3 ± 3.5	23	0.93 ± 0.07	56.6 ± 5.7	-
	AVA08B	L1106	2	161 ± 10	-	0.93 ± 0.07	174 ± 17	-
Central Amaz. (outcrop)	AVA22A	L1436	7	992 ± 133	29	1.08 ± 0.08	923 ± 142	152
	AVA22C	L1438	9	997 ± 92	32	0.86 ± 0.06	1167 ± 137	170
	AVA22E	L1440	4	1595 ± 275	27	1.52 ± 0.11	1058 ± 198	139
Central Amazonia (Autazes core)	155812	L1490	19	4.6 ± 0.5	44	3.96 ± 0.36	1.2 ± 0.2	-
	155813	L1491	12	94.6 ± 4.7	16	3.86 ± 0.36	24.6 ± 2.6	112
	155812	L1490	7	92.0 ± 8.8	21	3.96 ± 0.36	23.3 ± 3.1	-
	155813	L1491	6	237 ± 27	26	3.86 ± 0.36	61.6 ± 9.1	112
	155814	L1492	9	612 ± 76	38	3.99 ± 0.37	153 ± 24	180
	155815	L1493	7	504 ± 162	61	3.69 ± 0.35	137 ± 46	141
	155816	L1488	7	848 ± 76	24	2.53 ± 0.26	336 ± 46	130
	155817	L1487	12	834 ± 125	51	3.46 ± 0.33	242 ± 83	129
	155818	L1486	7	1096 ± 186	42	4.01 ± 0.38	274 ± 53	148
	155819	L1485	6	1692 ± 229	25	3.36 ± 0.34	505 ± 85	92

2.6 Discussion

2.6.1 TT-OSL equivalent doses and burial ages

TT-OSL ages obtained here can be interpreted as: i) the sand deposition age; ii) *in situ* weathering over older sedimentary fluvial deposits that give rise to soils, with the D_e representing the time since the last solar exposure due to soil mixing (Gray et al., 2020); or iii) the minimum age of the parent rock, because of the thermal instability or saturation of TT-OSL signals (Faershtein et al., 2018). Hence, the TT-OSL ages calculated for the different sandy substrates

may be interpreted as ages of sediment deposition, soil mixing processes, or an apparent age of quartz from the parent bedrock.

One of the main concerns when using the TT-OSL signal for sediment dating is its relatively low thermal stability (Chapot et al., 2016; Faershtein et al., 2018; Li and Li, 2006). A luminescence trap is considered thermally stable for periods lower than $\tau/10$ (where τ is the trap lifetime) (Aitken, 1998). The quartz OSL fast component, which is used for luminescence dating in the late Pleistocene and Holocene age range, has a trap lifetime of around 300 Ma at 10 °C (Jain et al., 2003; Singarayer and Bailey, 2003). Thus, it is considered stable in a million years (Ma) timespan and the maximum age limit is imposed by quartz OSL signal saturation. On the other hand, the TT-OSL main trap has a lifetime of 4 – 7 Ma at 10 °C to 20 °C (Adamiec et al., 2010; Faershtein et al., 2018; Shen et al., 2011; Thiel et al., 2012) or even lower, of 180 – 760 ka at 10 °C to 20 °C (Chapot et al., 2016; Li and Li, 2006), which would imply age limit in the hundred thousand years timespan due to thermal instability. Hence, thermal loss affects the TT-OSL signal in the Ma-scale age range, and even ages in the range of only a few hundred thousand years may be underestimated (Adamiec et al., 2010; Chapot et al., 2016; Faershtein et al., 2018; Shen et al., 2011). Another point for caution is the considerably slower rate of optical resetting of the TT-OSL signal compared with the fast OSL component. It might take weeks of natural sunlight exposure to deplete TT-OSL signals (e.g., Arnold et al., 2013; Demuro et al., 2015; Jacobs et al., 2011). These concerns should be addressed carefully. However, TT-OSL ages agree with independent age control in many cases (e.g., Arnold et al., 2015; Hernandez et al., 2015; Pickering et al., 2013), suggesting that quartz from different geological settings has an heterogenous behavior regarding TT-OSL thermal loss and bleaching suitability.

The calculated-to-given dose ratio of ~1.5 for the TT-OSL signal points to significant overestimation of D_e, possibly related to incomplete bleaching of the signal. This is also shown by the difference between OSL and TT-OSL D_e in the same samples, that ranges from 87 to 142 Gy, implying an overestimation of ~20-40 ka for Central Amazonia and of ~117 ka for Eastern Amazonia. TT-OSL signals bleach slower than the OSL signal, and they are not reduced to zero (Tsukamoto et al., 2008), having residual doses ranging from 5 to 40 Gy, depending on the depositional environment (Demuro et al., 2015; Duller and Wintle, 2012; Jacobs et al., 2011; Tsukamoto et al., 2008; Wang et al., 2006a). In the case of D_e relative to sedimentation ages, this implies that fluvial processes in lowland Amazonia are not enough for completely resetting the TT-OSL signal. If on one hand, there is overestimation of 20 to 117 ka due to residual doses, there might be an unaccounted for underestimation of the D_e due to the TT-OSL thermal instability.

Independent age control for the studied sediment samples from Central Amazonia is given by (U-Th)/He ages on supergene lateritic duricrusts and iron-enriched horizons within the Miocene-Pliocene fluvial sandstones (Gautheron et al., 2022) representing the substrate of the studied sandy

deposits. (U-Th)/He ages indicate that such sandstones were deposited and weathered in the last ~3 to 1 Ma (Gautheron et al., 2022). Therefore, the maximum depositional age of studied sandy substrates from Central Amazonia is from the late Pliocene and Pleistocene. This chronostratigraphic framework agrees with the interpretation of our TT-OSL ages as representing the timing of sediment deposition. Although the possibility of the TT-OSL ages indicating only the minimum age cannot be ruled out, considering the low thermal stability of TT-OSL signals (Chapot et al., 2016; Faershtein et al., 2018; Li and Li, 2006). Our TT-OSL ages ranging from almost 2 Ma matches other fluvial terraces of the Amazon River with TT-OSL depositional ages ranging from 556 to 1063 ka (Bezerra et al., 2022). The much younger OSL ages at the top of the Autazes core, from 1 to 25 ka, might represent the accumulation of fluvial sediments during major flooding events during the Late Pleistocene and Holocene (Pupim et al., 2019).

2.6.2 Geomorphic implications

OSL and TT-OSL ages constrain the formation of open and closed vegetation sandy substrates in lowland Amazonia, in both shallower and deeper profiles, extending the dated ages based on luminescence dating methods. The terraces dated previously using TT-OSL (Bezerra et al., 2022; Pupim et al., 2016) and the Autazes drill core (Kiefer et al., 2019) have both surface features and sedimentary structures that suggest fluvial deposition. However, many sandy terrains covered by savanna-like vegetation in lowland Amazonia lack surface depositional features or sedimentary structures, and correspond to massive, weathered sands covering Cretaceous-Paleogene and Miocene-Pliocene fluvial sandstones (Gautheron et al., 2022). The massive sandy constitution observed in the Eastern Amazonia and Central Amazonia open-vegetation sampling sites hinders the identification of a depositional or pedogenetic origin. The interpretation of TT-OSL ages as sediment deposition ages suggests fluvial systems with a higher base level and wider ancient floodplains across lowland Central and Eastern Amazonia during the Mid and Early Pleistocene. Fluvial sediments with Mid Pleistocene TT-OSL ages also were observed in terraces along the lower Xingu River (Pupim et al., 2016), eastward the study areas.

In Central Amazonia, after the deposition of these sandy terrains and their colonization by vegetation, their transformation into ‘white-sands’ occurred due to podzolization processes in the last ~1.2 Ma (sample AVA22C). Podzolization occurs by repeated rising and falling of the water table, which leaches organic matter and clays from the upper soil horizon, creating the light-colored sandy E horizon, and deposits them lower in the soil profile as the B horizon (Lundström et al., 2000). The main correlate for the white-sand ecosystems is the hydromorphic spodosols, occurring in the middle and upper Negro River basin (Adeney et al., 2016) and interpreted as *in situ* weathering of ancient deposits, like the Late Cretaceous sandstones of the Alter do Chão Formation (Horbe et al., 2004). Age constraints for deposition of substrates of these white-sand ecosystems are needed to appraise if spodosols developed over ancient sandstones, such as the

Late Cretaceous Alter do Chão Formation, or over Pleistocene sediments covering older rocky substrates. The first view implies the long-lasting occurrence of white-sand substrates beyond the Pleistocene while the second points to Pleistocene landscape shift driven by fluvial incision events followed by weathering of abandoned sandy deposits in uplands.

2.7 Conclusions

Quartz grains representative of lowland Amazonia sandy substrates colonized by open and closed vegetation ecosystems were used for SAR OSL and TT-OSL dating. The ages obtained in study sites of Central and Eastern Amazonia can represent the time of: (i) sediment deposition, (ii) soil mixing processes, or (iii) the minimum age of the weathered parent rock. Comparison between TT-OSL ages and (U-Th)/He ages from underlying iron crusts suggests that the sandy substrates can be formed by weathering of fluvial sediments accumulated during the Pleistocene, despite other interpretations cannot be ruled out. In Eastern Amazonia savanna sandy substrate, TT-OSL ages ranged from 1927 to 1239 ka. The Autazes core in Central Amazonia comprises heavily weathered fluvial sandstones and siltstones, covered by upland closed rainforest, with OSL ages from ~25 to 1 ka in the upper 2 m of the record. The OSL signal is saturated in downcore samples, where TT-OSL ages range from 505 to 23 ka ka until 14 m depth. TT-OSL ages obtained for the sandy substrate of WSE in Central Amazonia are in the 1167-923 ka range. The difference between OSL and TT-OSL ages for the same samples suggests that TT-OSL ages have an overestimation of ~20 ka to 117 ka. Assuming that the TT-OSL ages represent sediment deposition ages, we can interpret fluvial systems with a higher base level and wider floodplains in Central and Eastern Amazonia during the mid-Pleistocene. In this case, savanna and WSE in the study areas expanded over fluvial deposits during the Pleistocene.

Sample	Lab Code	N	D_e (Gy)	OD (%)	Dose rate (Gy/ka)	Age (ka)
AVA01C	L1083	7	562 ± 90	36	0.46 ± 0.08	1239 ± 294
AVA01E	L1084	7	713 ± 57	19	0.41 ± 0.04	1789 ± 237
AVA01G	L1085	8	747 ± 74	23	0.40 ± 0.03	1927 ± 246
AVA22A	L1436	7	992 ± 133	29	1.08 ± 0.08	923 ± 142
AVA22C	L1438	9	997 ± 92	32	0.86 ± 0.06	1167 ± 137
AVA22E	L1440	4	1595 ± 275	27	1.52 ± 0.11	1058 ± 198
155812	L1490	7	92.0 ± 8.8	21	3.96 ± 0.36	23.3 ± 3.1
155813	L1491	6	237 ± 27	26	3.86 ± 0.36	61.6 ± 9.1
155814	L1492	9	612 ± 76	38	3.99 ± 0.37	153 ± 24
155815	L1493	7	504 ± 162	61	3.69 ± 0.35	137 ± 46
155816	L1488	7	848 ± 76	24	2.53 ± 0.26	336 ± 46
155817	L1487	12	834 ± 125	51	3.46 ± 0.33	242 ± 83
155818	L1486	7	1096 ± 186	42	4.01 ± 0.38	274 ± 53
155819	L1485	6	1692 ± 229	25	3.36 ± 0.34	505 ± 85

2.8 References

Adamiec, G., Duller, G.A.T., Roberts, H.M., Wintle, A.G., 2010. Improving the TT-OSL SAR protocol through source trap characterisation. Radiat. Meas. 45, 768–777. https://doi.org/10.1016/j.radmeas.2010.03.009

Adeney, J.M., Christensen, N.L., Vicentini, A., Cohn-Haft, M., 2016. White-sand Ecosystems in Amazonia. Biotropica 48, 7–23. https://doi.org/10.1111/btp.12293

Aitken, M.J., 1998. Introduction to optical dating: the dating of Quaternary sediments by the use of photon-stimulated luminescence. Claredon Press.

Anderson, A.B., 1981. White-Sand Vegetation of Brazilian Amazonia. Biotropica 13, 199–210.

Arnold, L.J., Demuro, M., Navazo, M., Benito-Calvo, A., Pérez-González, A., 2013. OSL dating of the Middle Palaeolithic Hotel California site, Sierra de Atapuerca, north-central Spain. Boreas 42, 285–305. https://doi.org/10.1111/j.1502-3885.2012.00262.x

Arnold, L.J., Demuro, M., Parés, J.M., Pérez-González, A., Arsuaga, J.L., Bermúdez de Castro, J.M., Carbonell, E., 2015. Evaluating the suitability of extended-range luminescence dating techniques over early and Middle Pleistocene timescales: Published datasets and case studies from Atapuerca, Spain. Quat. Int. 389, 167–190. https://doi.org/10.1016/j.quaint.2014.08.010

Bezerra, I.S.A.A., Nogueira, A.C.R., Motta, M.B., Sawakuchi, A.O., Mineli, T.D., Silva, A. de Q., Silva, A.G., Domingos, F.H.G., Mata, G.A.T., Lima, F.J., Riker, S.R.L., 2022. Incision and aggradation phases of the Amazon River in central-eastern Amazonia during the late Neogene and Quaternary. Geomorphology 399, 108073. https://doi.org/10.1016/j.geomorph.2021.108073

Boubli, J.P., Ribas, C., Lynch Alfaro, J.W., Alfaro, M.E., da Silva, M.N.F., Pinho, G.M., Farias, I.P., 2015. Spatial and temporal patterns of diversification on the Amazon: A test of the riverine hypothesis for all diurnal primates of Rio Negro and Rio Branco in Brazil. Mol. Phylogenet. Evol. 82, 400–412. https://doi.org/10.1016/j.ympev.2014.09.005

Chapot, M.S., Roberts, H.M., Duller, G.A.T., Lai, Z.P., 2016. Natural and laboratory TT-OSL dose response curves: Testing the lifetime of the TT-OSL signal in nature. Radiat. Meas. 85, 41–50. https://doi.org/10.1016/j.radmeas.2015.11.008

Cremon, É.H., Rossetti, D. de F., Sawakuchi, A. de O., Cohen, M.C.L., 2016. The role of tectonics and climate in the late Quaternary evolution of a northern Amazonian River. Geomorphology 271, 22–39. https://doi.org/10.1016/j.geomorph.2016.07.030

Demuro, M., Arnold, L.J., Parés, J.M., Sala, R., 2015. Extended-range luminescence chronologies suggest potentially complex bone accumulation histories at the Early-to-Middle Pleistocene palaeontological site of Huéscar-1 (Guadix-Baza basin, Spain). Quat. Int. 389, 191–212. https://doi.org/10.1016/j.quaint.2014.08.035

Duller, G.A.T., 2003. Distinguishing quartz and feldspar in single grain luminescence measurements. Radiat. Meas. 37, 161–165. https://doi.org/10.1016/S1350-4487(02)00170-1

Duller, G.A.T., Wintle, A.G., 2012. A review of the thermally transferred optically stimulated luminescence signal from quartz for dating sediments. Quat. Geochronol. 7, 6–20. https://doi.org/10.1016/j.quageo.2011.09.003

Faershtein, G., Guralnik, B., Lambert, R., Matmon, A., Porat, N., 2018. Investigating the thermal stability of TT-OSL main source trap. Radiat. Meas. 119, 102–111. https://doi.org/10.1016/j.radmeas.2018.09.010

Frasier, C.L., Albert, V.A., Struwe, L., 2008. Amazonian lowland, white sand areas as ancestral regions for South American biodiversity: Biogeographic and phylogenetic patterns in Potalia (Angiospermae: Gentianaceae). Org. Divers. Evol. 8, 44–57. https://doi.org/10.1016/j.ode.2006.11.003

Gautheron, C., Sawakuchi, A.O., dos Santos Albuquerque, M.F., Cabriolu, C., Parra, M., Ribas, C.C., Pupim, F.N., Schwartz, S., Kern, A.K., Gómez, S., de Almeida, R.P., Horbe, A.M.C., Haurine, F., Miska, S., Nouet, J., Findling, N., Riffel, S.B., Pinna-Jamme, R., 2022. Cenozoic weathering of fluvial terraces and emergence of biogeographic boundaries in Central Amazonia. Glob. Planet. Change 212, 103815. https://doi.org/10.1016/j.gloplacha.2022.103815

Gray, H.J., Keen-Zebert, A., Furbish, D.J., Tucker, G.E., Mahan, S.A., 2020. Depth-dependent soil mixing persists across climate zones. Proc. Natl. Acad. Sci. U. S. A. 117, 8750–8756. https://doi.org/10.1073/pnas.1914140117

Guérin, G., Christophe, C., Philippe, A., Murray, A.S., Thomsen, K.J., Tribolo, C., Urbanova, P., Jain, M., Guibert, P., Mercier, N., Kreutzer, S., Lahaye, C., 2017. Absorbed dose, equivalent dose, measured dose rates, and implications for OSL age estimates: Introducing the Average Dose Model. Quat. Geochronol. 41, 163–173. https://doi.org/10.1016/j.quageo.2017.04.002

Guérin, G., Mercier, N., Adamiec, G., 2011. Dose-rate conversion factors: update. Anc. TL 29, 5–8.

Haffer, J., 1969. Speciation in Amazonian Forest Birds. Science (80-.). 165, 131–138.

Hernandez, M., Bahain, J.J., Mercier, N., Tombret, O., Falguères, C., Jaubert, J., 2015. Dating results on sedimentary quartz, bones and teeth from the Middle Pleistocene archaeological site of Coudoulous I (Lot, SW France): A comparative study between TT-OSL and ESR/U-series methods. Quat. Geochronol. 30, 493–497. https://doi.org/10.1016/j.quageo.2015.06.003

Hoorn, C., Wesselingh, F.P., ter Steege, H., Bermudez, M.A., Mora, A., Sevink, J., Sanmartin, I., Sanchez-Meseguer, A., Anderson, C.L., Figueiredo, J.P., Jaramillo, C., Riff, D., Negri, F.R., Hooghiemstra, H., Lundberg, J., Stadler, T., Sarkinen, T., Antonelli, A., 2010. Amazonia Through Time: Andean Uplift, Climate Change, Landscape Evolution, and Biodiversity. Science (80-). 330, 927–931. https://doi.org/10.1126/science.1194585

Horbe, A.M.C., Horbe, M.A., Suguio, K., 2004. Tropical Spodosols in northeastern Amazonas State, Brazil. Geoderma 119, 55–68. https://doi.org/10.1016/S0016-7061(03)00233-7

Jacobs, Z., Roberts, R.G., Lachlan, T.J., Karkanas, P., Marean, C.W., Roberts, D.L., 2011. Development of the SAR TT-OSL procedure for dating Middle Pleistocene dune and shallow marine deposits along the

southern Cape coast of South Africa. Quat. Geochronol. 6, 491–513. https://doi.org/10.1016/j.quageo.2011.04.003

Jain, M., Murray, A.S., Bøtter-Jensen, L., 2003. Characterisation of blue-light stimulated luminescence components in different quartz samples: Implications for dose measurement. Radiat. Meas. 37, 441–449. https://doi.org/10.1016/S1350-4487(03)00052-0

Kiefer, G.L.S., Uhlein, A., Fanton, J.J., 2019. O Depósito Potassífero De Autazes No Contexto Estratigráfico Da Bacia Do Amazonas. Geosci. = Geociências 38, 349–365. https://doi.org/10.5016/geociencias.v38i2.12857

Li, B., Li, S.H., 2006. Studies of thermal stability of charges associated with thermal transfer of OSL from quartz. J. Phys. D. Appl. Phys. 39, 2941–2949. https://doi.org/10.1088/0022-3727/39/14/011

Lundström, U.S., Van Breemen, N., Bain, D., 2000. The podzolization process. A review. Geoderma 94, 91–107. https://doi.org/10.1016/S0016-7061(99)00036-1

Murray, A.S., Wintle, A.G., 2000. Luminescence dating of quartz using an improved single-aliquot regenerative-dose protocol. Radiat. Meas. 32, 57–73. https://doi.org/10.1016/S1350-4487(99)00253-X

Pickering, R., Jacobs, Z., Herries, A.I.R., Karkanas, P., Bar-Matthews, M., Woodhead, J.D., Kappen, P., Fisher, E., Marean, C.W., 2013. Paleoanthropologically significant South African sea caves dated to 1.1-1.0 million years using a combination of U-Pb, TT-OSL and palaeomagnetism. Quat. Sci. Rev. 65, 39–52. https://doi.org/10.1016/j.quascirev.2012.12.016

Porat, N., Duller, G.A.T., Roberts, H.M., Wintle, A.G., 2009. A simplified SAR protocol for TT-OSL. Radiat. Meas. 44, 538–542. https://doi.org/10.1016/j.radmeas.2008.12.004

Prescott, J.R., Hutton, J.T., 1994. Cosmic ray contributions to dose rates for luminescence and ESR dating: Large depths and long-term time variations. Radiat. Meas. 23, 497–500. https://doi.org/10.1016/1350-4487(94)90086-8

Preusser, F., Chithambo, M.L., Götte, T., Martini, M., Ramseyer, K., Sendezera, E.J., Susino, G.J., Wintle, A.G., 2009. Quartz as a natural luminescence dosimeter. Earth-Science Rev. 97, 184–214. https://doi.org/10.1016/j.earscirev.2009.09.006

Pupim, F. do N., Sawakuchi, A.O., Mineli, T.D., Nogueira, L., 2016. Evaluating isothermal thermoluminescence and thermally transferred optically stimulated luminescence for dating of Pleistocene sediments in Amazonia. Quat. Geochronol. 36, 28–37. https://doi.org/10.1016/j.quageo.2016.08.003

Pupim, F.N., Sawakuchi, A.O., Almeida, R.P., Ribas, C.C., Kern, A.K., Hartmann, G.A., Chiessi, C.M., Tamura, L.N., Mineli, T.D., Savian, J.F., Grohmann, C.H., Bertassoli, D.J., Stern, A.G., Cruz, F.W., Cracraft, J., 2019. Chronology of Terra Firme formation in Amazonian lowlands reveals a dynamic Quaternary landscape. Quat. Sci. Rev. 210, 154–163. https://doi.org/10.1016/j.quascirev.2019.03.008

Ribas, C.C., Aleixo, A., Nogueira, A.C.R., Miyaki, C.Y., Cracraft, J., 2012. A palaeobiogeographic model for biotic diversification within Amazonia over the past three million years. Proc. R. Soc. B Biol. Sci. 279, 681–689. https://doi.org/10.1098/rspb.2011.1120

Rossetti, D.F., Cohen, M.C.L., Tatumi, S.H., Sawakuchi, A.O., Cremon, É.H., Mittani, J.C.R., Bertani, T.C., Munita, C.J.A.S., Tudela, D.R.G., Yee, M., Moya, G., 2015. Mid-Late Pleistocene OSL chronology in western Amazonia and implications for the transcontinental Amazon pathway. Sediment. Geol. 330, 1–15. https://doi.org/10.1016/j.sedgeo.2015.10.001

Shen, Z.X., Mauz, B., Lang, A., 2011. Source-trap characterization of thermally transferred OSL in quartz. J. Phys. D. Appl. Phys. 44. https://doi.org/10.1088/0022-3727/44/29/295405

Singarayer, J.S., Bailey, R.M., 2003. Further investigations of the quartz optically stimulated luminescence components using linear modulation. Radiat. Meas. 37, 451–458. https://doi.org/10.1016/S1350-4487(03)00062-3

Soares, E.A.A., Tatumi, S.H., Riccomini, C., 2010. OSL age determinations of Pleistocene fluvial deposits in Central Amazonia. An. Acad. Bras. Cienc. 82, 691–699. https://doi.org/10.1590/S0001-37652010000300017

Thiel, C., Buylaert, J.P., Murray, A.S., Elmejdoub, N., Jedoui, Y., 2012. A comparison of TT-OSL and post-IR IRSL dating of coastal deposits on Cap Bon peninsula, north-eastern Tunisia. Quat. Geochronol. 10, 209–217. https://doi.org/10.1016/j.quageo.2012.03.010

Tsukamoto, S., Duller, G.A.T., Wintle, A.G., 2008. Characteristics of thermally transferred optically stimulated luminescence (TT-OSL) in quartz and its potential for dating sediments. Radiat. Meas. 43, 1204–1218. https://doi.org/10.1016/j.radmeas.2008.02.018

Vandenberghe, D., De Corte, F., Buylaert, J.P., Kučera, J., Van den haute, P., 2008. On the internal radioactivity in quartz. Radiat. Meas. 43, 771–775. https://doi.org/10.1016/j.radmeas.2008.01.016

Wang, X.L., Lu, Y.C., Wintle, A.G., 2006a. Recuperated OSL dating of fine-grained quartz in Chinese loess. Quat. Geochronol. 1, 89–100. https://doi.org/10.1016/j.quageo.2006.05.020

Wang, X.L., Wintle, A.G., Lu, Y.C., 2006b. Thermally transferred luminescence in fine-grained quartz from Chinese loess: Basic observations. Radiat. Meas. 41, 649–658. https://doi.org/10.1016/j.radmeas.2006.01.001

Wintle, A.G., Murray, A.S., 2006. A review of quartz optically stimulated luminescence characteristics and their relevance in single-aliquot regeneration dating protocols. Radiat. Meas. 41, 369–391. https://doi.org/10.1016/j.radmeas.2005.11.001

3 Geological controls upon formation and distribution of open vegetation ecosystems in Amazonia

FERNANDA COSTA G. RODRIGUES et al.

3.1 Abstract

The evolution of Amazonian biota and its remarkable biodiversity are intricately linked to the evolution of the physical landscape and the different environments occurring within the biome. Open vegetation ecosystems, especially white-sand ecosystems (WSE) and savannas, have long been thought as key environments of biotic diversification in Amazonia. Both Amazonian savannas and WSE are associated to sandy substrates and the hypotheses about the origin, resilience and dynamics of the open vegetation sandy terrains vary regionally. In this paper, we address the issue between the distribution of Amazonian open vegetation ecosystems and characteristics of their physical landscape, represented by regional precipitation, relief and type and age of geological substrates. Open vegetation ecosystems in Amazonia can be divided as occurring in both highland and lowland areas. In the highlands, long-term exhumation and weathering of pre-Cenozoic processes render more stable areas over time. Whereas in lowland Amazonia, the rapidly changing landscape due to the fluvial and eolian systems dynamics can expand or retract open vegetation areas more frequently. The greater occurrence of savannas and WSE upon the extensive sandy alluvial plains in Negro and Branco Rivers basins are associated to high permeability and repeated rising and falling of the water table, favoring the development of spodosols in that area. OSL ages in WSE and savanna sandy substrates in central and eastern Amazonia range from 67.9 ka to 0.9 ka. These ages can be interpreted as sedimentation ages or solar resetting by soil processes. The wide distribution of OSL D_e values (from <1 to 52 Gy), and overall constancy in grain size statistics (mean and standard deviation), BOSL and TL sensitivities and Zr/Ti and Zr content suggests of homogenization via soil mixing. However, the possibility of such ages representing the depositional timing cannot be ruled out. TT-OSL ages from deeper layers in the same study area imply that these substrates were likely formed by weathering of fluvial sediments accumulated in the Pleistocene (2 Ma to 23 ka) and deposited upon older sedimentary units. The availability of sandy substrates supporting open vegetation ecosystems change in multiple spatiotemporal scales, and depends on local conditions, such as water table depth, surface elevation and primary sediment grain size, which can lead to decoupling between regional climate patterns and spatial distribution of open vegetation ecosystems

4 Final remarks

In this thesis, we investigated the origin, chronology and changing dynamics of sandy substrates supporting open vegetation ecosystems in Amazonia. The main focus was understanding the spatial distribution of open vegetation ecosystems and the geological controls of their sandy substrates, including the chronology and sand sources. The conclusions presented herein are based on a comprehensive review on the substrate origins of different open vegetation ecosystems in the Amazonia, OSL and TT-OSL geochronology and a suite of analytical methods to interpret sources and origins of sands (i.e., luminescence sensitivity, grain size, inorganic geochemistry and magnetic susceptibility). The main conclusions are highlighted below:

- Amazonian open vegetation ecosystems occur both in highland and lowland areas, where the processes forming such substrates greatly differ in timescales.
- In highland areas, long-term exhumation and weathering of pre-Cenozoic quartz-rich rocks give rise to more stable sandy soils over time.
- In lowland areas, alternation between sediment deposition by fluvial and/or eolian systems and weathering phases creates more dynamic open vegetation environments.
- Due to the more dynamic formation of sandy substrates in lowland Amazonia, open vegetation ecosystems developed upon these substrates can expand or retract at a faster pace (10^3 years) when compared to their counterparts in highland areas.
- The greater occurrence of savannas and WSE in the watersheds of the Negro and Branco rivers are associated to extensive sandy alluvial plains, and the development of spodosols upon them.
- Both OSL and TT-OSL ages can represent the time of: (i) sediment deposition, (ii) soil mixing processes, or (iii) the minimum age of the weathered parent rock.
- The comparison between TT-OSL ages from sandy substrates and (U-Th)/He ages from underlying iron crusts suggests that the sandy substrates in central and eastern Amazonia were formed by weathering of fluvial sediments accumulated during the Pleistocene (from 1927 to ~23 ka).
- In the case of TT-OSL ages representing depositional ages, this implies in fluvial systems with a higher base level and wider floodplains in central and eastern Amazonia during the mid-Pleistocene. Therefore, the open vegetation ecosystems developed upon such fluvial substrates also expanded during the Pleistocene.
- OSL ages more likely represent solar resetting by soil processes from 67.9 ka to 0.9 ka, even though sediment deposition cannot be ruled out in all cases.

- Soil mixing processes would lead to the overall constancy in grain size statistics (mean and standard deviation), BOSL and TL sensitivities and Zr/Ti and Zr content in sandy substrates. These substrates were likely formed by sands from local sources, implying minor sediment transport.
- The availability of sandy substrates changing in multiple spatiotemporal scales has important implications for the biota, once highland sandy terrains can work as refugia if lowland sandy terrains experience retraction due to the expansion of muddy floodplains associated to large rivers.

References

Adeney, J.M., Christensen, N.L., Vicentini, A., Cohn-Haft, M., 2016. White-sand Ecosystems in Amazonia. Biotropica 48, 7–23. https://doi.org/10.1111/btp.12293

Alonso, J.Á., 2002. Characteristic Avifauna of White-Sand Forests in Northern Peruvian Amazonia. Louisiana State University.

Alonso, J.Á., Metz, M.R., Fine, P.V.A., 2013. Habitat specialization by birds in Western Amazonian white-sand forests. Biotropica 45, 365–372. https://doi.org/10.1111/btp.12020

Anderson, A.B., 1981. White-Sand Vegetation of Brazilian Amazonia. Biotropica 13, 199–210.

Anhuf, D., Ledru, M.P., Behling, H., Da Cruz, F.W., Cordeiro, R.C., Van der Hammen, T., Karmann, I., Marengo, J.A., De Oliveira, P.E., Pessenda, L., Siffedine, A., Albuquerque, A.L., Da Silva Dias, P.L., 2006. Paleo-environmental change in Amazonian and African rainforest during the LGM. Palaeogeogr. Palaeoclimatol. Palaeoecol. 239, 510–527. https://doi.org/10.1016/j.palaeo.2006.01.017

Ayres, J.M., Clutton-Brock, T.H., 1992. River Boundaries and Species Range Size in Amazonian Primates. Am. Nat. 140, 531–537. https://doi.org/10.1086/285427

Bates, J.M., 2001. Avian diversification in Amazonia: evidence for historical complexity and a vicariance model for a basic diversification pattern. Divers. biológica e Cult. da Amaz. 119–137.

Bookhagen, B., Strecker, M.R., 2010. Modern Andean Rainfall Variation during ENSO Cycles and its Impact on the Amazon Drainage Basin. Amaz. Landsc. Species Evol. A Look into Past 224–241. https://doi.org/10.1002/9781444306408.ch14

Borges, S.H., 2004. Species poor but distinct: Bird assemblages in white sand vegetation in Ja?? National Park, Brazilian Amazon. Ibis (Lond. 1859). 146, 114–124. https://doi.org/10.1111/j.1474-919X.2004.00230.x

Borges, S.H., Cornelius, C., Moreira, M., Ribas, C.C., Conh-Haft, M., Capurucho, J.M., Vargas, C., Almeida, R., 2016. Bird Communities in Amazonian White-Sand Vegetation Patches: Effects of Landscape Configuration and Biogeographic Context. Biotropica 48, 121–131. https://doi.org/10.1111/btp.12296

Borges, S.H., Cornelius, C., Ribas, C.C., Almeida, R., Guilherme, E., Aleixo, A., Dantas, S., Santos, M.P., Moreira, M., 2015. What is the avifauna of Amazonian white-sand vegetation? Bird Conserv. Int. 26, 192–204. https://doi.org/10.1017/S0959270915000052

Borghetti, F., Barbosa, E., Ribeiro, L., Ribeiro, J.F., Walter, B.M.T., 2020. South American Savannas Origin, in: Scoging, P.F., Sankaran, M. (Eds.), Savanna Woody Plants and Large Herbivores. John Wiley & Sons Ltd., pp. 77–122.

Briceño, H.O., Schubert, C., 1990. Geomorphology of the Gran Sabana, Guayana Shield, southeastern Venezuela. Geomorphology 3, 125–141. https://doi.org/10.1016/0169-555X(90)90041-N

Bush, M.B., 1994. Amazonian Speciation: A Necessarily Complex Model. J. Biogeogr. 21, 5. https://doi.org/10.2307/2845600

Bush, M.B., De Oliveira, P.E., Colinvaux, P.A., Miller, M.C., Moreno, J.E., 2004. Amazonian paleoecological histories: One hill, three watersheds. Palaeogeogr. Palaeoclimatol. Palaeoecol. 214, 359–393. https://doi.org/10.1016/j.palaeo.2004.07.031

Bush, M.B., Oliveira, P.E. de, 2006. The rise and fall of the Refugial Hypothesis of Amazonian Speciation: a paleoecological perspective. Biota Neotrop. 6. https://doi.org/https://dx.doi.org/10.1590/S1676-06032006000100002

Capurucho, J.M.G., Cornelius, C., Borges, S.H., Cohn-Haft, M., Aleixo, A., Metzger, J.P., Ribas, C.C., 2013. Combining phylogeography and landscape genetics of Xenopipo atronitens (Aves: Pipridae), a white sand campina specialist, to understand Pleistocene landscape evolution in Amazonia. Biol. J. Linn. Soc. 110, 60–76. https://doi.org/10.1111/bij.12102

Caputo, M. V, 2011. Discussão sobre a Formação Alter do Chão e o Alto de Monte Alegre. Contrib. à Geol. da Amaz. volume 7, 7–23.

Carneiro Filho, A., Schwartz, D., Tatumi, S.H., Rosique, T., 2002. Amazonian paleodunes provide evidence for drier climate phases during the Late Pleistocence-Holocene. Quat. Res. 58, 205–209. https://doi.org/10.1006/qres.2002.2345

Carneiro Filho, A., Zinck, J.A., 1994. Mapping paleo-aeolian sand cover formations in the northern Amazon basin from TM images. ITC J. 270–282.

Carvalho, W.D. de, Mustin, K., 2017. The highly threatened and little known Amazonian savannahs. Nat. Ecol. Evol. 1, 3. https://doi.org/10.1038/s41559-017-0100

Cheng, H., Sinha, A., Cruz, F.W., Wang, X., Edwards, R.L., D'Horta, F.M., Ribas, C.C., Vuille, M., Stott, L.D., Auler, A.S., 2013. Climate change patterns in Amazonia and biodiversity. Nat. Commun. 4, 1411. https://doi.org/10.1038/ncomms2415

Colinvaux, P., 1987. Amazon diversity in light of the paleoecological record. Quat. Sci. Rev. 6, 93–114. https://doi.org/10.1016/0277-3791(87)90028-X

Colinvaux, P.A., De Oliveira, P.E., Bush, M.B., 2000. Amazonian and neotropical plant communities on glacial time-scales: The failure of the aridity and refuge hypotheses. Quat. Sci. Rev. 19, 141–169. https://doi.org/10.1016/S0277-3791(99)00059-1

Coutinho, M.G. da N., 2008. Geologia do Craton Amazônico, in: Província Mineral Do Tapajós: Geologia, Metalogenia e Mapa Previsional Para Ouro Em SIG. CPRM, Rio de Janeiro, pp. 15–31.

CPRM, 2014. Folha SA.20-Z-D Manaus: carta geológica 1:250.000.

CPRM, 2008. Mapa Geológico do Estado do Pará.

Cracraft, J., 1985. Historical Biogeography and Patterns of Differentiation within the South American Avifauna: Areas of Endemism. Ornithol. Monogr. 49–84. https://doi.org/10.2307/40168278

Cremon, É.H., Rossetti, D. de F., Sawakuchi, A. de O., Cohen, M.C.L., 2016. The role of tectonics and climate in the late Quaternary evolution of a northern Amazonian River. Geomorphology 271, 22–39. https://doi.org/10.1016/j.geomorph.2016.07.030

Crivellari, S., Chiessi, C.M., Kuhnert, H., Häggi, C., da Costa Portilho-Ramos, R., Zeng, J.Y., Zhang, Y., Schefuß, E., Mollenhauer, G., Hefter, J., Alexandre, F., Sampaio, G., Mulitza, S., 2018. Increased Amazon freshwater discharge during late Heinrich Stadial 1. Quat. Sci. Rev. 181, 144–155. https://doi.org/10.1016/j.quascirev.2017.12.005

Dino, R., Silva, O.B., Abrahão, D., 1999. Palynological and stratigraphic characterization of the Cretaceous strata from the Alter do Chão Formation, Amazonas basin, in: UNESP, Simpósio Sobre o Cretáceo Do Brasil and Simpósio Sobre El Cretácico de América Del Sur. pp. 557–565.

Dino, R., Soares, E.A.A., Antonioli, L., Riccomini, C., Nogueira, A.C.R., 2012. Palynostratigraphy and sedimentary facies of Middle Miocene fluvial deposits of the Amazonas Basin, Brazil. J. South Am. Earth Sci. 34, 61–80. https://doi.org/10.1016/j.jsames.2011.11.008

Eden, M.J., McGregor, D.F.M., 1992. Dynamics of the forest–savanna boundary in the Rio Branco–Rupununi region of northern Amazonia, in: Furley, P.A., Proctor, J., Ratter, J.A. (Eds.), The Nature and Dynamics of Forest–Savanna Boundaries. Chapman & Hall, London, pp. 77–89.

Eiten, G., 1986. The use of the term" savanna". Trop. Ecol. 27, 10–23.

Espinoza, J.C., Marengo, J.A., Ronchail, J., Carpio, J.M., Flores, L.N., Guyot, J.L., 2014. The extreme 2014 flood in south-western Amazon basin: The role of tropical-subtropical South Atlantic SST gradient. Environ. Res. Lett. 9. https://doi.org/10.1088/1748-9326/9/12/124007

FAO-Unesco, 1992. Soil Map of the World 1:5000000. https://doi.org/10.4324/9781315061610-15

Figueiredo, J., Hoorn, C., van der Ven, P., Soares, E., 2009. Late Miocene onset of the Amazon River and the Amazon deep-sea fan: Evidence from the Foz do Amazonas Basin. Geology 37, 619–622. https://doi.org/10.1130/G25567A.1

Fine, P.V.A., García-Villacorta, R., Pitman, N.C.A., Mesones, I., Kembel, S.W., 2010. A Floristic Study of the White-Sand Forests of Peru [1]. Ann. Missouri Bot. Gard. 97, 283–305. https://doi.org/10.3417/2008068

Garreaud, R., Vuille, M., Compagnucci, R., Marengo, J., 2009. Present-day South American climate. Palaeogeogr. Palaeoclimatol. Palaeoecol. 281, 180–195. https://doi.org/10.1016/j.palaeo.2007.10.032

Gómez Tapias, J., Schobbenhaus, C., Montes Ramírez, N.., 2019. Geological Map of South America 2019. Scale 1:5 000 000. Paris. https://doi.org/10.32685/10.143.2019.929

Govin, A., Chiessi, C.M., Zabel, M., Sawakuchi, A.O., Heslop, D., Hörner, T., Zhang, Y., Mulitza, S., 2014. Terrigenous input off northern South America driven by changes in Amazonian climate and the North Brazil Current retroflection during the last 250 ka. Clim. Past 10, 843–862. https://doi.org/10.5194/cp-10-843-2014

Gray, H.J., Keen-Zebert, A., Furbish, D.J., Tucker, G.E., Mahan, S.A., 2020. Depth-dependent soil mixing persists across climate zones. Proc. Natl. Acad. Sci. U. S. A. 117, 8750–8756. https://doi.org/10.1073/pnas.1914140117

Guimarães, J.T.F., Nogueira, A.C.R., Da Silva, J.B.C., Soares, J.L., Alves, R., Kern, A.K., 2015. Palynology of the middle miocene-pliocene Novo Remanso Formation, Central Amazonia, Brazil. Ameghiniana 52, 107–134. https://doi.org/10.5710/AMGH.08.09.2014.2245

Haffer, J., 1990. Avian species richness in tropical South America. Stud. Neotrop. Fauna Environ. 25, 157–183. https://doi.org/10.1080/01650529009360816

Haffer, J., 1985. Avian Zoogeography of the Neotropical Lowlands. Ornithol. Monogr. Neotrop. Ornithol. 113–146.

Haffer, J., 1969. Speciation in Amazonian Forest Birds. Science (80-.). 165, 131–138.

Haffer, J., Prance, G.T., 2001. Climatic forcing of evolution in Amazonia during the Cenozoic: On the refuge theory of biotic differentiation. Amazoniana 16, 579–607.

Hess, L.L., Melack, J.M., Affonso, A.G., Barbosa, C., Gastil-Buhl, M., Novo, E.M.L.M., 2015. Wetlands of the Lowland Amazon Basin: Extent, Vegetative Cover, and Dual-season Inundated Area as Mapped with JERS-1 Synthetic Aperture Radar. Wetlands 35, 745–756. https://doi.org/10.1007/s13157-015-0666-y

Hoffmann, G., Ramirez, E., Taupin, J.D., Francou, B., Ribstein, P., Delmas, R., Dürr, H., Gallaire, R., Simões, J., Scotterer, U., Stievenard, M., Werner, M., 2003. Coherent isotope history of Andean ice cores over the last century. Geophys. Res. Lett. 30, 1179. https://doi.org/10.1029/2002GL014870

Hoorn, C., Mosbrugger, V., Mulch, A., Antonelli, A., 2013. Biodiversity from mountain building. Nat. Geosci. 6, 154. https://doi.org/10.1038/ngeo1742

Hoorn, C., Wesselingh, F.P., 2010. Amazonia: landscape and species evolution, Amazonia, Landscape and Species Evolution: A Look into the Past. Blackwell Publishing. https://doi.org/10.1002/9781444306408.ch1

Horbe, A.M.C., Motta, M.B., de Almeida, C.M., Dantas, E.L., Vieira, L.C., 2013. Provenance of Pliocene and recent sedimentary deposits in western AmazÔnia, Brazil: Consequences for the paleodrainage of the Solimões-Amazonas River. Sediment. Geol. 296, 9–20. https://doi.org/10.1016/j.sedgeo.2013.07.007

House, J.I., Archer, S., Breshears, D.D., Scholes, R.J., 2003. Conundrums in mixed woody-herbaceous plant systems. J. Biogeogr. 30, 1763–1777. https://doi.org/10.1046/j.1365-2699.2003.00873.x

Huber, O., 1987. Neotropical savannas: Their flora and vegetation. Trends Ecol. Evol. 2, 67–71. https://doi.org/10.1016/0169-5347(87)90151-0

IBGE, 2006. Mapa de Solos do Brasil 1:5000000.

Jaramillo, C., Rueda, M.J., Mora, G., 2006. Cenozoic plant diversity in the neotropics. Science (80-.). 311, 1893–1896. https://doi.org/10.1126/science.1121380

Jarvis, A., Reuter, H.I., Nelson, A., Guevara, E., 2008. Hole-filled SRTM for the globe Version 4, available from the CGIAR-CSI SRTM 90m Database.

Kanner, L.C., Burns, S.J., Cheng, H., Edwards, R.L., 2012. High-Latitude Forcing of the South American Summer Monsoon During the Last Glacial. Science (80-.). 335, 570–573. https://doi.org/10.1126/science.1213397

Latrubesse, E.M., Cozzuol, M., da Silva-Caminha, S.A.F., Rigsby, C.A., Absy, M.L., Jaramillo, C., 2010. The Late Miocene paleogeography of the Amazon Basin and the evolution of the Amazon River system. Earth-Science Rev. 99, 99–124. https://doi.org/10.1016/j.earscirev.2010.02.005

Latrubesse, E.M., Nelson, B.W., 2001. Evidence for Late Quaternary aeolian activity in the Roraima-Guyana region. Catena 43, 63–80. https://doi.org/10.1016/S0341-8162(00)00114-4

Luebert, F., Muller, L.A.H., 2015. Effects of mountain formation and uplift on biological diversity. Front. Genet. 6, 154. https://doi.org/10.3389/fgene.2015.00054

Marengo, J.A., Nobre, C.A., Tomasella, J., Oyama, M.D., de Oliveira, G.S., de Oliveira, R., Camargo, H., Alves, L.M., Brown, I.F., 2008. The drought of Amazonia in 2005. J. Clim. 21, 495–516. https://doi.org/10.1175/2007JCLI1600.1

Marengo, J.A., Tomasella, J., Soares, W.R., Alves, L.M., Nobre, C.A., 2012. Extreme climatic events in the Amazon basin. Theor. Appl. Climatol. 107, 73–85. https://doi.org/10.1007/s00704-011-0465-1

Matos, M. V., Borges, S.H., d'Horta, F.M., Cornelius, C., Latrubesse, E., Cohn-Haft, M., Ribas, C.C., 2016. Comparative Phylogeography of Two Bird Species, *Tachyphonus phoenicius* (Thraupidae) and *Polytmus theresiae* (Trochilidae), Specialized in Amazonian White-sand Vegetation. Biotropica 48, 110–120. https://doi.org/10.1111/btp.12292

Mayle, F.E., Beerling, D.J., Gosling, W.D., Bush, M.B., 2004. Responses of Amazonian ecosystems to climatic and atmospheric carbon dioxide changes since the last glacial maximum. Philos. Trans. R. Soc. London. Ser. B Biol. Sci. 359, 499–514. https://doi.org/10.1098/rstb.2003.1434

Nelson, B.W., Ferreira, C.A.C., Da Silva, M.F., Kawasaki, M.L., 1990. Endemism centres, refugia and botanical collection density in Brazilian Amazonia. Nature 345, 714–716. https://doi.org/10.1038/345714a0

Pupim, F.N., Sawakuchi, A.O., Almeida, R.P., Ribas, C.C., Kern, A.K., Hartmann, G.A., Chiessi, C.M., Tamura, L.N., Mineli, T.D., Savian, J.F., Grohmann, C.H., Bertassoli, D.J., Stern, A.G., Cruz, F.W., Cracraft, J., 2019. Chronology of Terra Firme formation in Amazonian lowlands reveals a dynamic Quaternary landscape. Quat. Sci. Rev. 210, 154–163. https://doi.org/10.1016/j.quascirev.2019.03.008

Ribas, C.C., Aleixo, A., Nogueira, A.C.R., Miyaki, C.Y., Cracraft, J., 2012. A palaeobiogeographic model for biotic diversification within Amazonia over the past three million years. Proc. R. Soc. B Biol. Sci. 279, 681–689. https://doi.org/10.1098/rspb.2011.1120

Roddaz, M., Viers, J., Brusset, S., Baby, P., Hérail, G., 2005. Sediment provenances and drainage evolution

of the Neogene Amazonian foreland basin. Earth Planet. Sci. Lett. 239, 57–78. https://doi.org/10.1016/j.epsl.2005.08.007

Rossetti, D. de F., Gribel, R., Cohen, M.C.L., Valeriano, M. de M., Tatumi, S.H., Yee, M., 2019. The role of Late Pleistocene-Holocene tectono-sedimentary history on the origin of patches of savanna vegetation in the middle Madeira River, southwest of the Amazonian lowlands. Palaeogeogr. Palaeoclimatol. Palaeoecol. 526, 136–156. https://doi.org/10.1016/j.palaeo.2019.04.017

Rossetti, D.F., Bertani, T.C., Zani, H., Cremon, E.H., Hayakawa, E.H., 2012a. Late Quaternary sedimentary dynamics in Western Amazonia: Implications for the origin of open vegetation/forest contrasts. Geomorphology 177–178, 74–92. https://doi.org/10.1016/j.geomorph.2012.07.015

Rossetti, D.F., Cohen, M.C.L., Pessenda, L.C.R., 2017a. Vegetation change in southwestern amazonia (Brazil) and relationship to the late pleistocene and holocene climate. Radiocarbon 59, 69–89. https://doi.org/10.1017/RDC.2016.107

Rossetti, D.F., Cohen, M.C.L., Tatumi, S.H., Sawakuchi, A.O., Cremon, É.H., Mittani, J.C.R., Bertani, T.C., Munita, C.J.A.S., Tudela, D.R.G., Yee, M., Moya, G., 2015. Mid-Late Pleistocene OSL chronology in western Amazonia and implications for the transcontinental Amazon pathway. Sediment. Geol. 330, 1–15. https://doi.org/10.1016/j.sedgeo.2015.10.001

Rossetti, D.F., Gribel, R., Rennó, C.D., Cohen, M.C.L., Moulatlet, G.M., Cordeiro, C.L. de O., Rodrigues, E. do S.F., 2017b. Late Holocene tectonic influence on hydrology and vegetation patterns in a northern Amazonian megafan. Catena 158, 121–130. https://doi.org/10.1016/j.catena.2017.06.022

Rossetti, D.F., Zani, H., Cohen, M.C.L., Cremon, É.H., 2012b. A Late Pleistocene-Holocene wetland megafan in the Brazilian Amazonia. Sediment. Geol. 282, 276–293. https://doi.org/10.1016/j.sedgeo.2012.09.015

Rossetti, D.F., Zani, H., Cremon, É.H., 2014. Fossil megafans evidenced by remote sensing in the Amazonian wetlands. Zeitschrift für Geomorphol. 58, 145–161. https://doi.org/10.1127/0372-8854/2013/0118

Rull, V., 2008. Speciation timing and neotropical biodiversity: The Tertiary-Quaternary debate in the light of molecular phylogenetic evidence. Mol. Ecol. 17, 2722–2729. https://doi.org/10.1111/j.1365-294X.2008.03789.x

Rull, V., Huber, O., Vegas-Vilarrúbia, T., Señaris, C., 2019. Definition and characterization of the pantepui biogeographical province. Biodivers. Pantepui Pristine “Lost World” Neotrop. Guiana Highl. 3–32. https://doi.org/10.1016/B978-0-12-815591-2.00001-X

Sarmiento, G., 1984. The ecology of neotropical savannas. Harvard University Press, Cambridge, UK.

Sato, H., Kelley, D.I., Mayor, S.J., Martin Calvo, M., Cowling, S.A., Prentice, I.C., 2021. Dry corridors opened by fire and low CO2 in Amazonian rainforest during the Last Glacial Maximum. Nat. Geosci. 14, 578–585. https://doi.org/10.1038/s41561-021-00777-2

Schaefer, C., Dalrymple, J., 1995. Landscape evolution in Roraima, North Amazonia: plantation, paleosols

and paleoclimates. Zeitschrift fur Geomophologie New Fölge 39, 1–28.

Scholes, R.J., Archer, S.R., 1997. TREE-GRASS INTERACTIONS IN SAVANNAS. Annu. Rev. Ecol. Syst. 28, 517–544. https://doi.org/10.1146/annurev.ecolsys.28.1.517

Sinha, N.P.K., 1968. Geomorphic Evolution of the Northern Rupununi Basin, Guyana.

Sioli, H., 1984. The Amazon and its main affluents: Hydrography, morphology of the river courses. and river types, in: Sioli, Harald (Ed.), The Amazon, Monographiae Biologicae. Springer Netherlands, Dordrecht, pp. 85–126. https://doi.org/10.1007/978-94-009-6542-3

Teeuw, R.M., Rhodes, E.J., 2004. Aeolian activity in northern Amazonia: Optical dating of Late Pleistocene and Holocene palaeodunes. J. Quat. Sci. 19, 49–54. https://doi.org/10.1002/jqs.815

Van Der Hammen, T., Hooghiemstra, H., 2000. Neogene and Quaternary history of vegetation, climate, and plant diversity in Amazonia. Quat. Sci. Rev. 19, 725–742. https://doi.org/10.1016/S0277-3791(99)00024-4

Voicu, G., Bardoux, M., Stevenson, R., 2001. Lithostratigraphy, geochronology and gold metallogeny in the Northern Guiana Shield, South America: A review. Ore Geol. Rev. 18, 211–236. https://doi.org/10.1016/S0169-1368(01)00030-0

Vuille, M., Bradley, R.S., Werner, M., Healy, R., Keimig, F., 2003. Modeling δ 18 O in precipitation over the tropical Americas: 1. Interannual variability and climatic controls. J. Geophys. Res. 108, 4174. https://doi.org/10.1029/2001JD002038

Wentworth, C.K., 1922. A Scale of Grade and Class Terms for Clastic Sediments. J. Geol. 30, 377–392. https://doi.org/10.1086/622910

Wesselingh, F.P., Salo, J.A., 2006. A Miocene perspective on the evolution of the Amazonian biota. Scr. Geol. 439–458.

Yoon, J.H., Zeng, N., 2010. An Atlantic influence on Amazon rainfall. Clim. Dyn. 34, 249–264. https://doi.org/10.1007/s00382-009-0551-6

Zani, H., Rossetti, D.F., 2012. Multitemporal Landsat data applied for deciphering a megafan in northern Amazonia. Int. J. Remote Sens. 33, 6060–6075. https://doi.org/10.1080/01431161.2012.677865

Zhang, Y., Chiessi, C.M., Mulitza, S., Sawakuchi, A.O., Häggi, C., Zabel, M., Portilho-Ramos, R.C., Schefuß, E., Crivellari, S., Wefer, G., 2017. Different precipitation patterns across tropical South America during Heinrich and Dansgaard-Oeschger stadials. Quat. Sci. Rev. 177, 1–9. https://doi.org/10.1016/j.quascirev.2017.10.012

Zhou, J., Lau, K.M., 1998. Does a monsoon climate exist over South America? J. Clim. 11, 1020–1040. https://doi.org/10.1175/1520-0442(1998)011<1020:DAMCEO>2.0.CO;2

Zular, A., 2016. VARIAÇÕES DA ZONA DE CONVERGÊNCIA INTERTROPICAL E DO NÍVEL RELATIVO DO MAR DURANTE O QUATERNÁRIO TARDIO REGISTRADAS EM DEPÓSITOS EÓLICOS DO NORDESTE E NORTE DO BRASIL. Universidade de São Paulo.

Zular, A., Sawakuchi, A.O., Chiessi, C.M., d'Horta, F.M., Cruz, F.W., Demattê, J.A.M., Ribas, C.C., Hartmann, G.A., Giannini, P.C.F., Soares, E.A.A., 2019. The role of abrupt climate change in the formation of an open vegetation enclave in northern Amazonia during the late Quaternary. Glob. Planet. Change 172, 140–149. https://doi.org/10.1016/j.gloplacha.2018.09.006

Appendix 1

Supplementary material for "Extended-range luminescence dating of central and eastern Amazonia sandy terrains"; accepted for publication in Frontiers Special Volume "Landscape Evolution of the Tropical Regions: Dates, Rates and Beyond", on June 13rd, 2022.

Table S1: Data summary of dose recovery tests performed on quartz grains of the studied samples for the OSL SAR protocol.

Sample	**Aliquots**	**Preheat (ºC)**	**Cutheat (ºC)**	**Given dose (Gy)**	**Calculated-to-given dose ratio**	**Average recycling ratio**	**Average recuperation (%)**	**High temperature bleaching** (step 7 in Table 2 – OSL protocol)
L1490	3/4	240	200	5	0.95	0.93	0.39	Yes
L1490	4/4	220	180	5	0.97	0.99	0.16	Yes
L1490	4/4	200	160	5	0.94	0.96	0.68	Yes
L1490	4/4	240	200	5	0.97	1.03	3.36	No
L1490	3/4	220	180	5	0.97	1.04	3.40	No
L1490	4/4	200	160	5	0.99	1.04	2.48	No
L1490	2/4	240	200	10	0.97	1.06	1.72	No
L1490	4/4	200	160	10	0.99	1.01	2.40	No
L1490	2/4	240	200	30	0.99	1.02	1.68	No
L1490	3/4	200	160	30	0.92	1.02	1.35	No
L1490	4/4	240	200	50	0.90	1.03	0.79	No
L1490	4/4	200	160	50	0.93	1.03	1.65	No
L1485	2/3	220	220	50	0.99	1.02	3.91	No
L1485	2/3	240	220	50	0.99	1.04	3.76	No
L1485	3/3	260	220	50	0.97	1.00	2.89	No

Table S2: Data summary of dose recovery tests performed on quartz grains of the studied samples for the TT-OSL SAR protocol. *Data from Bezerra et al. (2022).

Sample	**Aliquots**	**Preheat (ºC)**	**Cutheat (ºC)**	**Given dose (Gy)**	**Calculated-to-given dose ratio**	**Average recycling ratio**	**Average recuperation (%)**
L1088	3/3	260	200	200	1.40	0.88	0.47
L1088	2/3	260	200	400	1.40	0.81	0.26
P14-RT-B (TT-OSL)*	3/3	260	220	400	1.84	1.04	0.08
P14-RT-B (TT-OSL)*	3/3	260	220	1000	1.41	1.04	0.00

Table S3: Summary of dose rate data. "LOD" is limit of detection.

Location	Sample	Lab Code	Water saturation	U (ppm)	Th (ppm)	K (%)	Cosmic dose rate (Gy/ka)	β dose rate (Gy/ka)	γ dose rate (Gy/ka)
Eastern Amazonia (outcrop)	AVA01C	L1083	0.0205	0.368 ± 0.020	2.465 ± 0.105	0.011 ± 0.002	0.186 ± 0.075	0.109 ± 0.014	0.158 ± 0.018
	AVA01E	L1084	0.0218	0.278 ± 0.019	2.290 ± 0.103	< LOD	0.174 ± 0.037	0.087 ± 0.011	0.138 ± 0.016
	AVA01G	L1085	0.0158	0.299 ± 0.017	2.088 ± 0.090	0.009 ± 0.002	0.163 ± 0.025	0.092 ± 0.012	0.133 ± 0.016
	AVA08B	L1106	0.0050	0.762 ± 0.035	8.200 ± 0.273	0.007 ± 0.003	0.158 ± 0.022	0.290 ± 0.037	0.477 ± 0.056
Central Amazonia (outcrop)	AVA22A	L1436	0.0192	3.490 ± 0.124	1.128 ± 0.090	< LOD	0.178 ± 0.024	0.464 ± 0.059	0.454 ± 0.050
	AVA22C	L1438	0.0334	2.624 ± 0.101	1.191 ± 0.161	0.004 ± 0.002	0.163 ± 0.016	0.353 ± 0.045	0.338 ± 0.039
	AVA22E	L1440	0.0383	4.460 ± 0.123	4.900 ± 0.173	< LOD	0.151 ± 0.013	0.655 ± 0.080	0.702 ± 0.078
Central Amazonia (core)	155812	L1490	0.0078	6.590 ± 0.461	30.100 ± 3.010	0.080 ± 0.008	0.191 ± 0.016	1.586 ± 0.217	2.178 ± 0.289
	155813	L1491	0.0085	5.890 ± 0.412	31.550 ± 3.155	0.080 ± 0.008	0.156 ± 0.011	1.528 ± 0.209	2.167 ± 0.290
	155814	L1492	0.0086	5.990 ± 0.419	33.700 ± 3.700	0.100 ± 0.007	0.139 ± 0.010	1.591 ± 0.218	2.255 ± 0.303
	155815	L1493	0.0077	5.690 ± 0.398	30.410 ± 3.041	0.080 ± 0.008	0.107 ± 0.008	1.478 ± 0.203	2.093 ± 0.281
	155816	L1488	0.0136	0.410 ± 0.019	30.210 ± 3.021	0.220 ± 0.015	0.097 ± 0.007	0.902 ± 0.131	1.524 ± 0.223
	155817	L1487	0.0128	4.030 ± 0.282	30.550 ± 3.055	0.270 ± 0.019	0.088 ± 0.006	1.407 ± 0.191	1.952 ± 0.264
	155818	L1486	0.0040	4.470 ± 0.313	32.360 ± 3.236	0.580 ± 0.041	0.056 ± 0.004	1.760 ± 0.237	2.184 ± 0.294
	155819	L1485	0.0103	3.100 ± 0.217	35.550 ± 3.550	0.080 ± 0.008	0.046 ± 0.003	1.261 ± 0.178	2.045 ± 0.286